ChemTexts (2022) 8:5
https://doi.org/10.1007/s40828-021-00156-9

LECTURE TEXT

Risk assessment and remediation of NAPL contaminated soil and groundwater

Stephen Leharne[1]

Received: 1 February 2021 / Accepted: 1 December 2021 / Published online: 27 December 2021

Abstract

The presence of water-immiscible organic liquids—commonly called non-aqueous phase liquids or NAPLs—in soils and groundwater, is a worldwide environmental problem. Typical examples of NAPLs include: petroleum products, organic solvents and organic liquid waste from laboratories and industry. The molecular components of NAPLs present in soils, rocks and groundwater are readily transferred to the vapour and aqueous phases. The extent to which they do this is determined by their solubility (which is quite limited) and vapour pressure (which can be quite high). These molecular components, once dispersed in the vapour phase or dissolved in the aqueous phase, can provide a long-term source of harm to biotic receptors. The object of this lecture text is to examine how we can assess the degree of harm using quantitative risk assessment and how NAPL contaminated environments can be restored through the use of chemical, biological and physical remediation technologies.

Graphical abstract

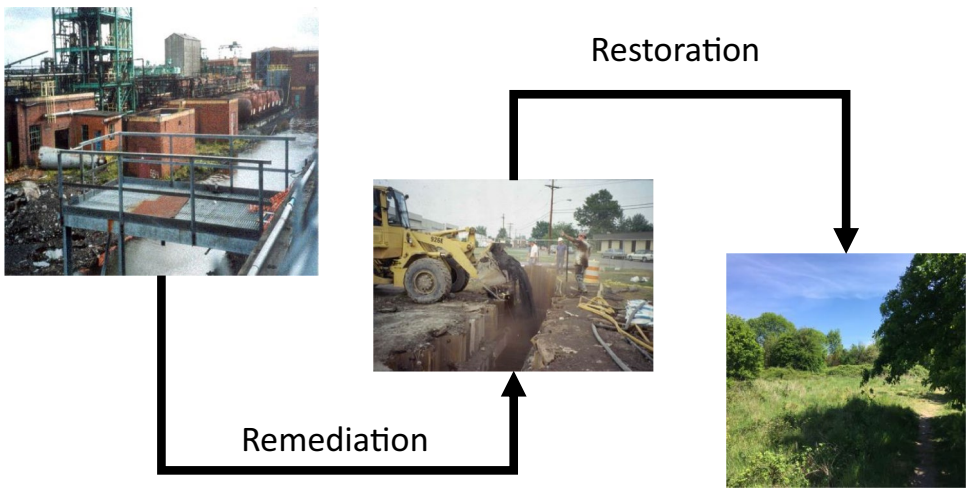

Keywords NAPLs · Remediation · Risk assessment

Introduction

A wide variety of water-immiscible organic liquids—referred to as non-aqueous phase liquids (NAPLs)—have been manufactured and used since the beginning of the twentieth century [1]. Commonly encountered examples include chlorinated hydrocarbon solvents, coal tar products

✉ Stephen Leharne
S.A.Leharne@gre.ac.uk

[1] Faculty of Engineering and Science, University of Greenwich, Pembroke, Chatham Maritime, Kent ME4 4TB, UK

and petroleum. In a previous manuscript [2] we examined the environmental behaviour and fate of NAPLs in the sub-surface environment. It was noted that NAPLs are released into the environment through inappropriate or careless use, storage in leaking containers and pipes (see Fig. 1), spillage or inappropriate disposal.

In the this text it is important to draw the reader's attention to an important point regarding terminology. NAPL refers to the separate phase organic liquid. Most NAPLs encountered in the environment are liquid mixtures of several components. These components are able to transfer to the vapour phase by vaporisation or the aqueous phase by solubilisation. When molecularly dispersed in the vapour or aqueous phase they are no longer referred to as NAPLs but as NAPL components. In fact the term VOC (volatile organic compound) is sometimes used to describe the molecularly dispersed components in the vapour phase. In this text we shall use the term VOC as shorthand for a NAPL component that is either dissolved in water or present in the vapour phase.

When a NAPL is discharged into the soil environment it will tend to migrate vertically downwards towards the water table. NAPLs readily displace air in the unsaturated sub-surface—this is the sub-surface zone where pore spaces contain either air or water. NAPLs, however, do not necessarily displace water. This is because of the capillary forces generated at the curved interface between water and NAPL in the pore network, which is of capillary dimensions. See Ref. [2] for further details.

On the trailing edge of a migrating NAPL body, droplets of NAPL are detached and are trapped in the pore space. These droplets are immobile. Capillary forces are responsible for the trapping of these droplets, which are commonly referred to as residuals. NAPL bodies of sufficient volume will, at some stage, come into contact with the saturated zone. This is the sub-surface zone where all pore spaces are filled with water. NAPLs that are denser than water can penetrate the saturated zone if they are able to overcome the capillary forces generated at the water/NAPL interface. NAPLs with a density less than that of water will accumulate above the water table.

Fig. 1 Coal tar NAPL leaking from a broken pipe in a former coking works

The presence of NAPL in the sub-surface may pose a serious threat of harm to environmental receptors (be they animal, plant or abiotic) via the vapour and aqueous phases. NAPL in the unsaturated zone can vaporise directly into the vapour phase, which in turn can dissolve into infiltrating rain water, which will eventually contaminate groundwater. NAPL in the saturated zone directly contaminates groundwater through solubilisation and can contaminate the unsaturated zone through volatilisation—the transfer of a solute from the aqueous phase to the vapour phase. NAPL components present in either phase are then readily transported by advection from the NAPL source zone to the "at-risk" receptor.

Important questions immediately arise when NAPL is present in the subsurface:

- Does the presence of NAPL or NAPL components (VOCs) in the subsurface environment necessarily provide a risk of harm to a receptor? Or, is there a threshold below which no harm is anticipated? If so, how can we determine this threshold?
- How can we quantify the probability and scale of harm? We call this process risk assessment.
- If risk assessment demonstrates the probability of substantial harm, how can we ameliorate that harm?
- Finally, when can intervention to remediate a contaminated site be shown to have reduced the risk of harm to acceptable levels? That is, when can we stop our remedial works?

The purpose of this manuscript is therefore: (1) to examine the basics of environmental risk assessment, which for our purposes will examine some basic aspects of environmental modelling, coupled with exposure assessment and the use of toxicological data, and (2) following on from this, to examine the variety of (bio)chemical/engineering processes that have been proposed to remediate these contaminated environments, with a particular emphasis upon the underlying chemistry and physics.

Risk assessment

Quantitative environmental risk assessment involves the application of a number of characterisation procedures. For substances that do not cause cancer, risk assessment includes the following stages [3].

Hazard characterisation

Animal studies or epidemiology can provide a dose level below which no adverse effects are anticipated. Dose normally has the units of mg (of toxicant) per kg (of receptor body weight) per day. In general, animal studies are designed to reveal the chemical dose rate at which either a **n**o **o**bserved **a**dverse **e**ffects **l**evel (**NOAEL**), or a minimal observed adverse effects level (**L**owest **OAEL**), is observed. NOAELs or LOAELs are then divided by uncertainty factors to account for the following:

- intra-human variability—some humans may be more sensitive than others to the toxicant;
- inter-species variability—the test animals may be less sensitive than humans to the toxicant;
- and if using a LOAEL we need to reduce it to a NOAEL [4].

The numerical values of the uncertainty factors are normally set by toxicological experts, who work for a particular organisation or committee, charged with providing occupational and/or environmental exposure limits to selected environmental contaminants [4]. The end result of using these uncertainty factors is a toxicant dose rate below which we should not observe any health problems. This dose may be referred to as the tolerable daily intake (TDI), the reference dose (RfD) or human limit value (HLV).

Exposure assessment

For this stage, uptake via various exposure routes is calculated. These routes may include breathing contaminated air, eating contaminated food or drinking contaminated water. It is usual to have some fixed assumptions as to the quantities per day of water drunk, air inhaled, and soil/dust or food ingested [5].

Risk characterisation

The last stage involves comparing the calculated daily dose obtained in the exposure assessment stage with the TDI. If it is greater, then some remedial intervention may be required.

Risk assessment calculations

A typical example of how toxicological data can be converted into a safe soil concentration is provided by Pohl and co-workers [6]. Their work was concerned with assessing non-cancer risks associated with exposure to 2,3,7,8-tetrachlorodibenzene-*p*-dioxin (TCDD).

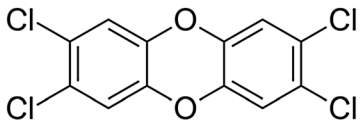

2,3,7,8-tetrachlorodibenzene-*p*-dioxin

Dioxins, it should be noted, have no marketable industrial uses and are usually found as unwanted by-products of industrial and combustion processes [7]. For example, 2,3,7,8-tetrachlorodibenzene-*p*-dioxin was produced in small quantities during the production of 2,4,5-trichlorophenol. The phenol was manufactured by the alkaline hydrolysis of 1,2,4,5-tetrachlorobenzene, and 2,3,7,8-tetrachlorodibenzene-*p*-dioxin was formed via the dimerization of the phenol [7].

Pohl et al. used data from an investigation that reported that a 14-day acute (a short time period) exposure to doses—ranging from 0.01 to 2.0 μg kg^{-1} day^{-1}—of TCDD suppressed serum total haemolytic complement activity in female B6C3F1 mice [8]. Complement proteins are part of the immune system that aid in the destruction of bacteria in alliance with antibodies [9]. It was found that TCDD increases susceptibility to *Streptococcus pneumoniae*, a bacterial pathogen whose host defence is complement mediated [8]. Since even the lowest dose rate used in the study of 0.01 μg kg^{-1} day^{-1} suppressed serum total haemolytic complement activity, this dose is identified as a LOAEL. From this Pohl et al. derived a TDI by dividing the LOAEL by the following uncertainty factors:

- 10 for using a LOAEL—they assumed that reduction of the lowest dose rate by an order of magnitude would convert a LOAEL to NOAEL.
- 10 for extrapolation from animals to humans—they assumed that the animals could be less susceptible to the toxicant than humans.
- and 10 for intra-human variability—they assumed that some humans might be more susceptible than others. Thus, the calculated TDI value obtained in the second stage might only protect some humans [6].

They also divided by a modifying factor of 0.5 because the TCDD was administered in a more bioavailable form (it was dissolved in oil) than it would be if it were administered absorbed in soil. Thus, the acute TDI for TCDD was calculated to be:

$$\frac{0.01\ (\mu g\ kg^{-1}\ day^{-1})}{10\times 10\times 10\times 0.5} = 20\ (pg\ kg^{-1}\ day^{-1}).$$

This is an extremely small dose rate and confirms just how toxic TCDD is. This TDI was then converted into a safe soil level by assuming that a normal person ingests 100 mg of soil per day and that their body weight is 70 kg [6]. A safe soil level was then calculated using the formula:

$$\text{Safe soil concentration} = \frac{\text{TDI} \times \text{BW}}{I_{\text{rate}}}, \quad (1)$$

where TDI is the tolerable daily intake (pg kg^{-1} day^{-1}), BW is body weight (kg) and I_{rate} is the ingestion rate of soil (g day^{-1}).

A dimensional analysis readily shows that the result of using the formula shown in Eq. (1) is a safe soil concentration.

$$\frac{\frac{\text{pg of TCDD}}{\text{kg body weight} \times \text{day}} \times \text{kg body weight}}{\frac{\text{g of soil}}{\text{day}}} = \frac{\text{pg of TCDD}}{\text{g of soil}}.$$

We can convert the units of the final safe soil concentration to more frequently encountered units by using conversion factors (such as 10^{-6} $\mu g\ pg^{-1}$); these are used in the following calculation:

$$\frac{20\ (pg\ kg^{-1}\ day^{-1}) \times 70\ (kg) \times 10^{-6}\ (\mu g\ pg^{-1})}{100\ (mg\ day^{-1}) \times 10^{-3}\ (g\ mg^{-1})} = 0.014\ (\mu g\ g^{-1}).$$

This value would normally be quoted as 14 ppb (parts per billion), which is equivalent to 14 ng g^{-1}.

There are several aspects of the analysis that we need to appreciate.

- The dose rate may not be protective of human health for chronic (long-term) exposure [6]. Indeed, for chronic exposure Pohl et al. [6] have suggested that a lower dose rate of 0.7 pg kg^{-1} day^{-1} should be used. This translates into a safe soil concentration of 0.5 ppb, which should protect human receptors from ill effects arising from chronic exposure.
- Children are at greater risk of harm for two reasons. First, their body weights are smaller. Pohl et al. assume that the average child body weight is 10 kg [6]. Second, children probably consume greater quantities of soil (assumed to be 200 mg day^{-1}) [6] through contaminated hand to mouth activity. So whilst the established safe dose rate does not change, the safe soil concentration does change, if we consider children to be the critical receptors. For them the safe soil concentration, derived from acute exposure data, would be:

$$\frac{20\ (pg\ kg^{-1}\ day^{-1}) \times 10\ (kg) \times 10^{-6}\ (\mu g\ \ pg^{-1})}{200\ (mg\ \ day^{-1}) \times 10^{-3}\ (g\ \ mg^{-1})} = 0.001\ (\mu g\ \ g^{-1})$$

or 1 ppb—14 times lower than the adult safe soil level. The safe level used would be determined by circumstances. The higher level would possibly be used if the critical receptors were workers who were occupationally exposed. The lower value may be used if the soil under investigation was present in a children's play area.

The reader at this point will begin to appreciate that it is of critical importance to understand the assumptions that underpin the setting of a safe soil level so that it can be applied appropriately.

Cancer risk assessment

So far we have examined toxicological outcomes that do not result in cancer; as a result we have been able to establish thresholds below which we are confident that no ill effects will result from a specified exposure dose rate. On the other hand, it is usually assumed that there is no safe threshold dose for carcinogenic (having the potential to cause cancer) materials.

The response observed for a population exposed to a carcinogen are dichotomous and probabilistic. By dichotomous we mean that result of exposure is either yes—with cancer—or no—without cancer [10]. If the exposure dose rate is low and the time period over which exposure occurs is small then the number of cancers is likely to be very low. If the dose rate and/or the time period of exposure increases then the probability of increased cancers occurring in the population will increase. We thus need a way of assessing cancer risk that considers the time scale over which cancer may develop as a result of exposure to a carcinogen and the fact that the outcome of exposure is probabilistic. What we mean by this latter statement is that we cannot really make an assessment about whether an individual will develop cancer as a result of exposure to a carcinogen. We can only make an assessment about the excess cancers we may see developing in an exposed population.

Cancer risk assessment is therefore based upon animal studies or epidemiological studies that compute the number of excess cancers that appear in an exposed population compared to the number of cancers that appear in an non-exposed population. The purpose of animal studies is to examine the relationship between the number of excess cancers as a function of dose. The number of excess cancers can be converted into the empirical probability (or relative frequency) of cancer and is then plotted against dose. The data can then be fitted to a model and in the linear low-dose

region of the fit the slope can be measured giving the so-called slope factor [5]. The slope factor essentially gives the cancer risk in an exposed population to a dose rate of 1 mg kg^{-1} day^{-1}. Epidemiological studies on the other need to be able to calculate doses in occupationally exposed populations—this would involve estimates of exposure time and concentrations—and correlate these figures with the empirical probability of excess cancers. This, as may be expected, is very hard to accomplish.

The models used to fit the data should be based upon a sound conceptual understanding of how cancer is initiated and progresses. Unfortunately, the theory is not well developed and so the models used to fit the data are empirical [10]. Most models are constructed based upon a mathematical description of what are believed to be the elementary underlying biological mechanisms [11]. The animal studies will generally be based upon the application of large doses to observe statistically significant occurrences of cancer, in the exposed population, over a specified timespan [5]. The models will then be chosen so as to give a non-threshold linear response (the slope factor) in the low dose region [12] as shown, indicatively, in Fig. 2. The low dose region encompasses the range of exposure values over which we might expect to see a population exposed.

We can examine how we use cancer slope factors in risk assessments by considering the following example.

Problem: tetrachloromethane in drinking water (adapted from Ref. [5])

Tetrachloromethane (TCM) is a DNAPL (a NAPL which is denser than water), which is slightly soluble in water (0.846 g dm^{-3} at 25 °C [13]). TCM has been discovered in the drinking water supplied to a city of 500,000 at a concentration of 7.3 μg dm^{-3}. The oral cancer slope factor for TCM is 7×10^{-2} (mg kg^{-1} $day^{-1})^{-1}$ [14]. What is the cancer risk associated with drinking this water?

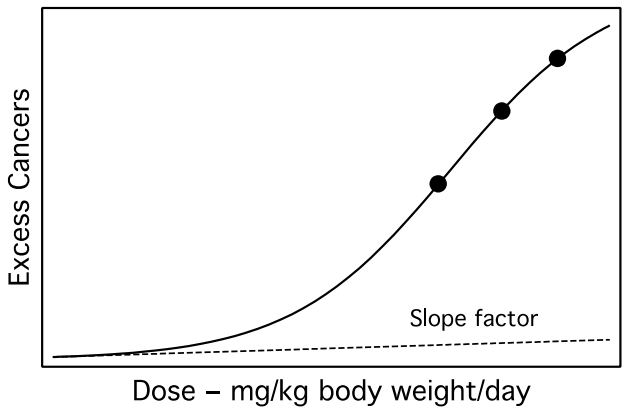

Fig. 2 Indicative dose response relationship for a carcinogen showing how extrapolation to low doses provides a linear region which provides the slope factor

To answer this question we assume that adult humans consume 2 l of water per day over their lifetime (of 70 years) and that the bodyweight of an adult is 70 kg [5]. Thus, the chronic daily intake *(CDI)*—the daily intake of a toxicant averaged over a life time—is given by:

$$\mathrm{CDI} = \frac{C_w \times \mathrm{IR}}{\mathrm{BW}}, \tag{2}$$

where C_w is the aqueous concentration of TCM (μg dm^{-3}), IR is the ingestion rate of water (dm^3 day^{-1}) and BW is bodyweight (kg)

$$\frac{7.3\left(\frac{\mu g}{dm^3}\right) \times 2\left(\frac{dm^3}{day}\right) \times 10^{-3}\left(\frac{mg}{\mu g}\right)}{70\ (\mathrm{kg})} = 0.00021\left(\frac{\mathrm{mg}}{\mathrm{kg\ day}}\right).$$

The equation contains the factor—10^{-3} (mg μg^{-1})—which is used to covert the CDI to the correct dose units of mg kg^{-1} day^{-1}.

The cancer risk is then obtained by multiplying the cancer slope factor with the chronic daily intake.

$$\text{Cancer risk rate} = \text{Cancer slope factor} \times \text{CDI} \tag{3}$$

$$7 \times 10^{-2}\left(\frac{\mathrm{mg}}{\mathrm{kg\ day^{-1}}}\right)^{-1} \times 0.00021\left(\frac{\mathrm{mg}}{\mathrm{kg\ day^{-1}}}\right) = 14.6 \times 10^{-6}.$$

The cancer risk is 14.6×10^{-6}, which signifies that we would expect to see 14.6 excess cancers in a population of 1 million exposed daily to this level of TCM in their drinking water over a 70-year period (the assumed exposure lifetime). The yearly excess cancer rate for a population of 500,000 drinking this water daily would work out to be:

$$5 \times 10^5\ (\text{persons}) \times \frac{14.6\ (\text{excess cancers})}{10^6\ (\text{persons})} \times \frac{1}{70\ (\text{years})},$$

which is approximately 0.1 excess cancers per year or about 1 excess cancer every 9.6 years. The number of new cancers per year for the UK is reported to be 367,167 [15]. The population of the UK is 66.65 million, which suggests that in a city of 500,000 we should expect about 2750 new cancers a year. A figure of 0.1 excess cancers per year resulting from drinking TCM-contaminated water is thus unlikely to be detected.

We can calculate a concentration value which would be protective of the population using 1×10^{-6} as an acceptable risk level [5]. Equation (3) can be rearranged to give an acceptable daily intake (ADI):

$$\mathrm{ADI} = \frac{\text{Acceptable cancer risk level}}{\text{Cancer slope factor}} \tag{4}$$

$$\mathrm{ADI} = \frac{10^{-6}}{7 \times 10^{-2}\left(\frac{\mathrm{mg}}{\mathrm{kg \times day}}\right)^{-1}} = 1.43 \times 10^{-5}\left(\frac{\mathrm{mg}}{\mathrm{kg \times day}}\right).$$

Again assuming that average human weighs 70 kg and consumes 2 l of water per day then the ADI is converted into a safe water concentration in the following way:

$$\text{Safe water concentration} = \frac{\mathrm{ADI}\left(\frac{\mathrm{mg}}{\mathrm{kg \times day}}\right) \times \text{Body weight (kg)}}{\text{Water ingestion rate}\left(\frac{\mathrm{dm^3}}{\mathrm{day}}\right)}$$

$$\frac{1.43 \times 10^{-5}\left(\frac{\mathrm{mg}}{\mathrm{kg \times day}}\right) \times 70\ (\mathrm{kg})}{2\left(\frac{\mathrm{dm^3}}{\mathrm{day}}\right)} = 5 \times 10^{-4}\left(\frac{\mathrm{mg}}{\mathrm{dm^3}}\right) \rightarrow 0.5\left(\frac{\mu g}{\mathrm{dm^3}}\right).$$

The US EPA enforcement limit for TCM in water is 5 μg dm^{-3}, which may reflect the technical infeasibility of trying to enforce a lower limit or the use of a higher acceptable risk level.

It is worth noting that trichloromethane may be detected in drinking water as a result of disinfection using chlorine [16]. Disinfection is a very necessary step in ensuring that drinking water does not contain dangerous pathogens. Thus, anyone making a risk assessment would need to balance the need to effectively disinfect water against the cancer risk.

Problem: benzene in the indoor environment

The concentration of benzene in groundwater below a dwelling is 189 μg m^{-3}. What is the concentration of benzene in the interior environment of the dwelling? Figure 3 shows a conceptual model that we can use to examine the problem. Benzene in the sub-surface aqueous phase is in equilibrium with benzene in the sub-surface vapour phase. Benzene-laden air migrates from the soil vapour phase into the home at the rate of 10 m^3 h^{-1}. The house is estimated to have a volume of 500 m^3. It is a well-mixed environment, i.e. the concentration of benzene is homogeneous throughout the interior. The air change rate (ACR)—the fraction of the indoor air that is replaced per hour—is 0.3 h^{-1}. It is assumed that the concentration of benzene in the exterior ambient atmospheric compartment is negligible. Thus, the only source of benzene in the house is groundwater.

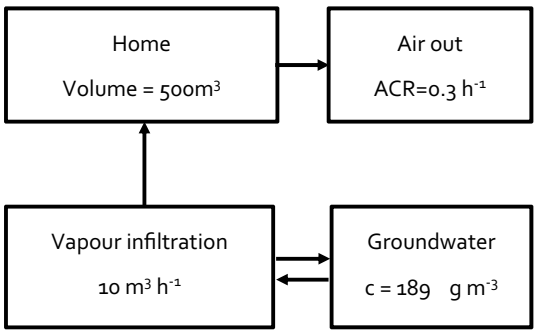

Fig. 3 Conceptual model for the infiltration of benzene into the indoor environment

To answer this problem we assume that the distribution of benzene between the aqueous and vapour phases is thermodynamically controlled. The equilibrium distribution of a compound between the aqueous and gaseous phases is described by the Henry's law constant. It may be recalled that Raoult's law expresses the relationship between the vapour pressure of a component and its concentration in a liquid mixture as:

$$p_i = x_i p_i^* \tag{5}$$

where p_i is the vapour pressure of component i in equilibrium with a liquid mixture, x_i is the mole fraction of component i in the liquid phase and p_i^* in the saturated vapour pressure of component i. A plot of p_i against x_i is linear with the slope equal to p_i^* for an ideal solution. In the Henry's law region where the concentration of i is extremely small, a similar plot is also linear but the gradient is not equal to p_i^* [17]. Instead, the gradient is referred to as the Henry's law constant (H) and functions as a partition coefficient.

$$H = \frac{p_i}{x_i}. \tag{6}$$

McKay uses an alternative form of the Henry's law equation [18]:

$$H' = \frac{p_i}{c_i}, \tag{7}$$

where p_i is the partial pressure of the compound and c_i is the solubility of the compound in water. This equation itself can be used to provide a dimensionless partition equation by dividing through by RT where R is the universal gas constant and T is the absolute temperature:

$$\frac{H'}{RT} = \frac{\frac{p_i}{RT}}{C_i} \rightarrow K_{\mathrm{aw}} = \frac{C_{\mathrm{a}}}{C_{\mathrm{w}}}, \tag{8}$$

K_{aw} for benzene is 0.22 [18].

To solve the problem we assume that: (1) the indoor concentration of benzene is at a steady state and (2) the house interior is well mixed so that the concentration is constant in all the interior air space. We can thus formulate a steady-state mass balance equation where the rate at which benzene enters the building is balanced by the rate of removal by ventilation.

$$C_{\text{Soil air}}\left(\frac{\mu g}{m^3}\right) \times \text{IFR}\left(\frac{m^3}{h}\right) = C_{\text{Indoor air}}\left(\frac{\mu g}{m^3}\right) \times \text{ACR}\left(\frac{1}{h}\right) \times V_{\text{Indoor air}}\ (m^3), \tag{9}$$

where $C_{\text{Soil air}}$ and $C_{\text{Indoor air}}$ are the concentrations of benzene in soil air and indoor air respectively. The ventilation rate is denoted by ACR, which is the air change rate and is defined as the fraction of indoor air that is exchanged with fresh air every hour. IFR is the infiltration rate and is a measure of the volume of soil air entering the building per hour. Finally, $V_{\text{Indoor air}}$ is the volume of air in the building. Using Eq. (8) we can rewrite Eq. (9) to give:

$$\begin{aligned} &K_{aw} \times C_{\text{Water}} \times \text{IFR} = C_{\text{Indoor air}} \times \text{ACR} \times V_{\text{Indoor air}} \\ &0.22 \times 189\ (\mu g\ \ m^{-3}) \times 10\ (m^3\ h^{-1}) = C_{\text{Indoor air}} \times 0.3\ (h^{-1}) \times 500\ (m^3) \\ &C_{\text{Indoor air}} = 2.77\ (\mu g\ \ m^{-3}). \end{aligned} \tag{10}$$

The inhalation unit risk associated with benzene is 2.2×10^{-6} $(\mu g\ m^{-3})^{-1}$ [19]. This figure is the expected number of excess cancers in a population of 1 million who have been exposed over a lifetime to a dose of 1 $\mu g\ m^{-3}$. The cancer risk is therefore:

$$2.77\ (\mu g\ \ m^{-3}) \times 2.2 \times 10^{-6}\ (\mu g\ \ m^{-3})^{-1} = 6.1 \times 10^{-6},$$

which is greater than 1×10^{-6}, the putative acceptable risk level [5]. An acceptable atmospheric concentration can be calculated using the inhalation unit risk:

$$\frac{10^{-6}}{2.2 \times 10^{-6}\ (\mu g\ \ m^{-3})^{-1}} = 0.45\ (\mu g\ \ m^{-3}),$$

which, in the outlined scenario, translates into an acceptable aqueous concentration of 30.7 $\mu g\ m^{-3}$. Interestingly, this value is very much less than the WHO guideline value of 1 $\mu g\ dm^{-3}$ or 1 $mg\ m^{-3}$ for drinking water [20], which demonstrates that site-specific risk assessments may require more diligence than the simple application of guideline values [21].

Risk linkage: source pathway receptor

Harm may occur when a receptor is exposed to a hazardous material via one or more exposure pathways. The protection of a receptor requires that the connection that links a source containing a hazardous material and the pathway by which the hazardous material is transferred to a receptor must be broken. For NAPLs it is therefore of paramount importance to identify the source and the particular routes by which NAPL and/or its molecularly dispersed components in the subsurface environment pose unacceptable risks to identified receptors.

A NAPL source zone can be defined as:

> "…a saturated or unsaturated subsurface zone containing hazardous substances, pollutants, or contaminants"…derived from a NAPL "…that acts as a reservoir that sustains a contaminant plume in groundwater, surface water, or air, or acts as a source for direct exposure" [22].

NAPL source zones may contain:

1. Pooled NAPL—which is potentially mobile given an external pressure stimulus.
2. NAPL trapped in pore spaces by capillary forces as droplets or ganglia, which are immobile under normal water flow conditions.
3. NAPL components encountered as vapour and water phase contaminants and ad/absorbed to organic matter present on solid surfaces.
4. Dissolved NAPL components may also diffuse into the matrix of porous rocks and remain there for a considerable time. Indeed, when the NAPL has been fully

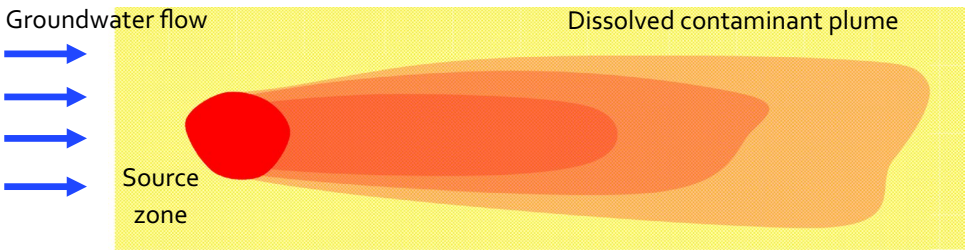

Fig. 4 Plan view cartoon showing the development of a contaminant plume in groundwater. The gradation in colour is intended to represent the differences in VOC concentration in the plume. The darker the colour the higher the concentration

depleted, back-diffusion from the rock matrix will occur thereby prolonging the lifetime of the source zone.

NAPL components in the source zone dissolve into flowing groundwater or vaporise into the soil air to create a plume of contamination as shown in Fig. 4. The plume develops in the direction of groundwater flow in the aqueous phase and in the direction of the barometric pressure gradient in the vapour phase. Plume development is described by the advection dispersion equation [23, 24]:

$$\frac{\partial c}{\partial t} = -v\frac{\partial c_{\mathrm{w}}}{\partial x} + D\left(\frac{\partial^2 c_{\mathrm{w}}}{\partial x^2}\right) + \frac{\rho_{\mathrm{B}}}{\phi}\frac{\partial c_{\mathrm{s}}}{\partial t} + \frac{\partial c_{\mathrm{w}}}{\partial t}, \tag{11}$$

where c_{w} is the aqueous phase concentration of VOC (ML^{-3}), t is time (T), v is the transport velocity—the rate at which water flows ($\mathrm{L\ T}^{-1}$), x is distance along the longitudinal direction of the plume (L), D is the longitudinal dispersion coefficient ($\mathrm{L}^2\ \mathrm{T}^{-1}$), ρ_{B} is the bulk density of the sub-surface environment (ML^{-3}), ϕ is the porosity of the sub-surface environment (–), and c_{s} is the amount of VOC sorbed per unit mass of solid (–).

The first term on the right-hand side of Eq. (11) is the advective term and describes the transport of solute in the flowing aqueous phase. The term is negative because the flow of solute is from the high concentration source zone away to some point downgradient from the source zone where the concentration is lower. Thus, the concentration gradient is negative. The second term, on the right-hand side, refers to dispersion, which describes the spreading of the contaminant plume from regions of high-to-low solute concentration. The dispersion term is made of contributions from: diffusion—the mass transfer at the molecular level of solute molecules from high to low concentration and hydrodynamic dispersion—which arises from the fact that a fluid, and thus the entrained dissolved VOC, (1) moves faster through the centre of pores than at the sides, (2) moves along different pathways through a porous medium some of which are comparatively long and some of which are shorter and (3) travels faster through large pores than through smaller pores. Dispersion is three dimensional and as such occurs longitudinally, in the direction of transport, laterally (transverse dispersion) and vertically. Longitudinal dispersion is normally greater than lateral dispersion. The two may, however, be approximately equal when flow rates through porous media are very small [25]. Equation (11), as written, is one dimensional, and D refers to longitudinal dispersion only.

Advective transport is retarded by sorption to stationary solid surfaces. This is described by the third term on the right-hand side of the equation. In the subsurface organic solute transport is usually retarded by ad/absorption to organic matter. The final term, on the right-hand side, describes the abiotic and/or biotic degradation of the VOC.

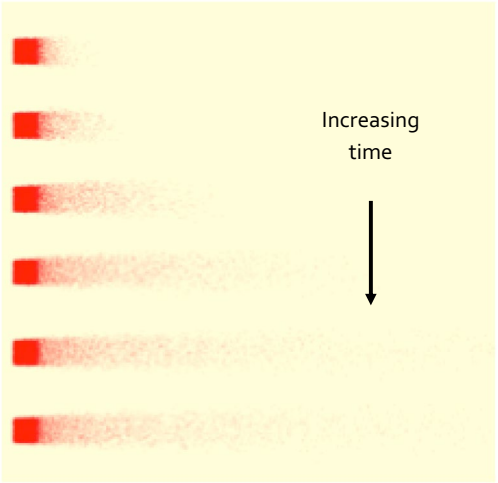

Fig. 5 Formation of a steady-state plume. The diagram is shown in plan view—i.e. looking down on the system

If we use the simple stochastic model that we introduced into the previous publication [2], we can show that plume development does not go on indefinitely. In fact, the plume will come to a steady state where the rate of solute dissolution is balanced by the rates of dispersion and degradation. Under steady-state conditions the plume length remains constant. This is shown in Fig. 5, which neatly demonstrates that the concentration of solute in the plume varies with distance from the source. Essentially the concentration is at its highest closest to the source and increasingly lower the further away from the source. At some point in the longitudinal direction from the source, the concentration is lower that the detection limit of the analytical method.

Problems arise when a contaminant plume intersects a regulatory compliance point. This could be one of the following:

- A public water supply borehole. This will result in the public being exposed to the contaminant through contaminated drinking water. Risk assessment will determine if the level of exposure will result in adverse health outcomes.
- Streams, rivers and lakes. These surface water features are fed by groundwater. If the plume intersects surface water then risk assessment will determine whether there will be adverse health outcomes for both sediment and water dwelling organisms.
- Migration of the plume across a property boundary. Off-site migration of the plume under buildings can result in contamination of indoor air through volatilisation. Again quantitative risk assessment will determine whether exposure will result in adverse health outcomes.

The owner of a site where such a contaminant source is located will assume, in most jurisdictions, liability for the harm caused and will be compelled to prevent further harm.

If the source remains in place then the plume is sustained and the harm continues. If the source is removed then the problem should eventually be resolved. However, the principal and very often complex problem is trying to locate the plume source. The ground surface location of a spill does not necessarily supply information on the sub-surface location of the source. Kueper et al. [1] have shown that NAPLs in the sub-surface spread as they downwardly migrate. The depth of migration is dependent upon the structure of the sub-surface. For example, spreading occurs when the downwardly migrating NAPL meets a capillary barrier [1] such as a water-saturated fine-grained silt or clay layer. The pressure needed to overcome the capillary forces generated at the NAPL/water interface at the tight junctions formed by the particles comprising the layer is large and given by the following inequality [2]:

$$P_{\mathrm{N}} > P_{\mathrm{w}} + \frac{2\sigma \mathrm{Cos}\,(\theta)}{r}, \tag{12}$$

where P is the pressure (units Pa) exerted by the NAPL (N) and water (w) phases, respectively, σ is the water/NAPL interfacial tension (units N m^{-1}), θ is the contact angle (dimensionless) and r is the pore throat radius (units m)—the pore throat is the junction of two more grains that form the entry point into a pore. If the NAPL cannot penetrate the capillary barrier, it will, then, spread across the barrier.

NAPL will also readily migrate in the contiguous network of fractures found in sub-surface rocks as long as the fracture apertures are of a suitable size. NAPL bodies of sufficient mass can migrate far and deep in fractured rock environments.

Thus, source removal whilst attractive is not necessarily easy to accomplish since the source may well be difficult to locate. For some NAPLs like coal tar, which has a density close to that of water and is highly viscous, migration is extremely slow. In such cases soil excavation has been used to remedy the problem, though the problem as to what to do with the excavated soil remains. On the other hand chlorinated hydrocarbons, which have a substantially greater density than that of water and a much lower viscosity, migrate extremely quickly and in a direction determined by the structure and heterogeneity of the sub-surface.

How long will a NAPL source zone remain a hazard to health?

To answer this question we could ask two ancillary questions:

1. For how long does NAPL remain in the source zone as a separate phase?
2. For how long does water coming from the source zone provide a risk of harm to environmental receptors?

To answer question 1 we could consider the following problem. If the source zone is solely comprised of a single component free phase NAPL then we could use the following equation:

$$\frac{\mathrm{d}M}{\mathrm{d}t} = -SQ, \tag{13}$$

where M is the NAPL mass (M), t is time (T), S is solubility (ML^{-3}) and Q is the volumetric flow of water ($L^3\ T^{-1}$). Equation (13) assumes that the NAPL and water are in intimate contact and that the solubilisation of the NAPL is not kinetically limited. Integration of Eq. (13) gives:

$$\int_{M_0}^{M} \mathrm{d}M = -SQ \int_{0}^{t} \mathrm{d}t \rightarrow M = M_0 - SQt, \tag{14}$$

Removal of TCM as a separate phase corresponds to $M = 0$ and thus Eq. (14) after some rearrangement provides an expression for the time to full depletion:

$$t = \frac{M_0}{SQ}. \tag{15}$$

Let's consider a direct leak of 60 L of trichloromethane (TCM) into groundwater. Let's assume that the TCM source zone forms a rectangular prism of dimensions 0.5 m (height) × 0.5 m (width) × 4 m (length). The total volume of the rectangular prism is 1 m^3. Let's assume that the porosity of the system is 0.3. Porosity is the volume of pore space divided by the total volume of the system. Thus, the volume of pore space is 0.3 m^3, which means that the source zone is 20% saturated with TCM which is a reasonable figure. Let's assume that the source zone is located in fine sand, which has a relatively homogeneous grain size (hydrogeologists describe such a system as well sorted). The hydraulic conductivity of the sand is 1×10^{-5} m s^{-1} and hydraulic gradient is 0.01 (see [2] for further explanation of these terms).

Using the Darcy's law equation [24], we can obtain Q:

$$Q = AK_{\mathrm{H}}\frac{\Delta h}{\Delta l}, \tag{16}$$

where A is the cross-sectional area through which flow occurs (L^2), K_H is the hydraulic conductivity ($L\ T^{-1}$) and $\Delta h/\Delta l$ is the hydraulic gradient.

In our example the cross-sectional area is $0.5\ m \times 0.5\ m = 0.25\ m^2$. Thus, the volumetric flow-through is:

$$Q = 0.25\ (m^2) \times 1 \times 10^{-5} \left(\frac{m}{s}\right) \times 0.01 = 2.5 \times 10^{-8} \left(\frac{m^3}{s}\right),$$

or $0.0022\ m^3\ day^{-1}$. The solubility of TCM is $8.09\ g\ dm^{-3}$ [18] and the density of TCM is $1479\ g\ L^{-1}$ [26]. The initial mass of TCM, M_0, is 88.74 kg, and the time necessary to remove the TCM as a separate phase is 5078 days or about 13.8 years.

It is important to stress the assumptions that drive this result. We assume that the source zone behaves, in chemical engineering terms, as a continuously stirred (well-mixed) reactor and that the solubilisation of TCM in water is driven purely by thermodynamics. Since the source zone is at equilibrium, the chemical potential of the dissolved TCM (μ_{aq}) and the chemical potential of the TCE NAPL phase (μ_N) are equal. Using the standard expression for chemical potential written in terms of the standard chemical potential (μ°) and chemical activity (a) [17] and assuming TCM is a single component with no impurities, we can write:

$$\begin{aligned} &\mu_N = \mu_{aq} \\ &\mu_N^o + RT \ln a_N = \mu_{aq}^o + RT \ln a_{aq} \\ &\text{since } a_N = 1 \text{ and } a_{aq} \approx S \\ &\text{and } \mu_{aq}^o - \mu_N^o = \Delta G^o \\ &\frac{\Delta G^o}{RT} = -\ln S, \end{aligned} \tag{17}$$

which leads to the result that the equilibrium constant is the solubility of TCM (S in Eq. 17). As TCM-laden water leaves the source zone and is replaced by clean water, Le Chatelier's principle is obeyed and equilibrium is instantaneously restored through further dissolution of TCM; since the source zone is a continuously stirred reactor the concentration of TCM in water is constant throughout the source zone and is equal to the solubility of TCM.

Kinetically, the removal of TCM dissolved in water is a zero order process when TCM NAPL is present since the concentration of dissolved TCM in the outflow water from the source zone is controlled by its solubility which is time invariant. However, once TCM as a separate phase disappears, dissolved TCM, which is still present in the source zone, will now be removed from the source zone by a first-order kinetic process.

We can explain why this is the case by using the conceptual model presented in Fig. 6. The volume of water present in the source zone is V_w. The volume of water flowing through the source zone in unit time (i.e. the flow-rate) is Q. Thus, the fraction of water flowing out per unit time is $\frac{Q}{V_w}$, which has the units of T^{-1} and is a first-order rate. The expression $\frac{Q}{V_w} C_w$ describes the mass of dissolved TCM that is removed in unit time.

The removal process can be described by the following kinetic expression:

$$\frac{dC_w}{dt} = -\frac{Q}{V_w} C_w, \tag{18}$$

which on integration and rearrangement gives

$$C = C_0 e^{-\frac{Q}{V_w} t}. \tag{19}$$

The concentration of TCM in groundwater emerging from the source zone can then be given by the following piecewise expression:

$$C(t) = \begin{cases} S & t < t_{dis} \\ Se^{-\frac{Q}{V_w} t} & t \geq t_{dis} \end{cases}, \tag{20}$$

where t_{dis} is the time for the TCM to disappear as a separate NAPL phase, which is given by Eq. (15). The USEPA has set a safe water concentration for TCM of $0.08\ mg\ dm^{-3}$ [27]. The time necessary for the outflow concentration to reach this level is 28.4 years. Thus, even when the NAPL has disappeared as a separate phase the problem still persists for a further 14.6 years.

If we accept the assumptions that were made to facilitate the calculation then it becomes immediately apparent that the architecture of the source zone is an important factor controlling the time to depletion. For instance, if the

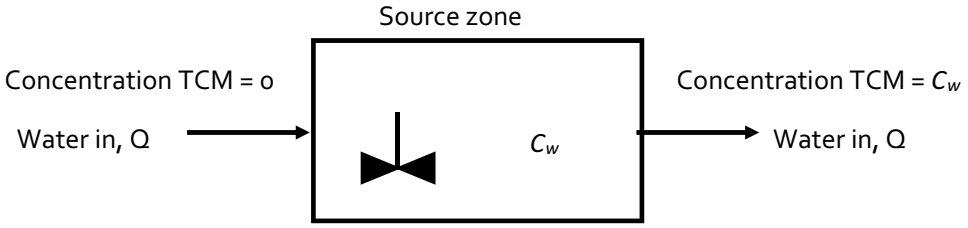

Fig. 6 Conceptual model of dissolved TCM removal from the source zone once TCM NAPL has been finally removed. The paddle symbol indicates that the system is well mixed

cross-sectional area was an order of magnitude smaller and the length of the source zone correspondingly bigger, then the time to reduce the TCM concentration in the outflow to below the USEPA safe level would be about 285 years. Identifying the location and architecture of the source zone is clearly an important but unfortunately difficult forensic engineering problem.

So far, we have assumed that the source zone is at thermodynamic equilibrium. This is implied by the assumption that the aqueous phase in the source zone is always saturated with VOC. In other words, we assume that there are no time constraints upon the attainment of saturation. Unfortunately environmental systems rarely—if ever—exist in thermodynamic equilibrium. It is therefore common for measured VOC concentrations in groundwater to be a factor of 10 or more lower than their pure phase solubility [28]. The reason for this is due to kinetic constraints placed on the mass transfer of VOC molecules from the NAPL to the aqueous phase by molecular diffusion [28].

For the source zone where a NAPL derived VOC is distributed between the contacting NAPL and aqueous phases, thermodynamic equilibrium is achieved when the chemical potential of the compound is equal in both phases. For this to occur the aqueous phase concentration of the VOC in the source zone must be homogeneous. The concentration however is only likely to be homogeneous if the system is agitated. In groundwater, agitation can be provided by turbulence, which arises when the inertial forces (forces associated with momentum) that give rise to flow are very much greater than the viscous forces that oppose flow [29]. However, groundwater turbulence is unlikely to arise in subsurface media that are finer than coarse gravels [29]. Thus, for our model system, which is comprised of fine sand, it means that water flow through the source zone is likely to be laminar.

What is laminar flow? Laminar flow is characterised by fluid particles moving smoothly along flow paths in layers. Each layer moves at a slightly different velocity compared to its neighbouring layers. Those layers closest to a stationary solid surface move slowest. Indeed, the layer next to the stationary surface (called the boundary layer) is itself stationary, whilst those further away move increasingly more quickly. The further they are from the stationary surface, the faster they move. Most importantly there is no lateral mixing between adjacent layers. Thus, VOC molecules that have migrated from the NAPL phase to the aqueous phase can only spread by molecular diffusion since no other mixing mechanism exists. If the flow rate is increased sufficiently then turbulence is introduced. Turbulence is demonstrated by the appearance of eddies or vortices. These will significantly improve mass transfer.

Diffusive mass transfer is described by Fick's first law of diffusion:

$$J = -DA\frac{\Delta c}{\Delta x} \tag{21}$$

J (M T^{-1}) is the rate at which material diffuses down a concentration gradient $\Delta c/\Delta x$ (M L^{-4})—where c is concentration and x is length—through a fluid of cross-sectional area, A (L^2). D is the diffusion coefficient (dimensions L^2 T^{-1}). Note the presence of the negative sign on the right-hand side of this equation. This arises because the concentration gradient is negative. The diffusive mass transfer of matter proceeds from a high to a low concentration in a single medium such as water. Since the concentration gets smaller with distance from the source zone, the concentration gradient is negative.

It is common to combine the diffusion coefficient (D) and Δx—the length over which the concentration difference is measured into one parameter—the mass transfer coefficient (L T^{-1}), which has the units of velocity. In fact, we can go further and combine D, A and Δx into a lumped parameter, k_w (L^3 T^{-1}). The product of the lumped parameter and concentration has the units of M T^{-1}.

We assume that the concentration of the VOC on the water side of the NAPL/water interface is either:

- equal to the solubility for a single component NAPL or
- is given by Raoult's Law—$S_i^* x_i$ where S_i^* is the solubility of the pure phase and x_i is the mole fraction of component i for a mixed component NAPL.

To make things simpler, we shall assume that diffusion only takes place across the boundary layer. The rest of the aqueous phase is well mixed through turbulence.

Two equations can be written which describe the change in mass in each compartment. For the NAPL phase the change in mass of TCM with time is a balance between the flux rate of TCM from the NAPL body into water ($-k_w S$) and the flux rate of TCM from water back into the NAPL body ($k_w C_w$):

$$\frac{dm}{dt} = k_w (C_w - S), \tag{22}$$

where m is the mass of TCM, t is time, C_w is the aqueous phase concentration of TCM and S is the solubility of TCM in water.

For the water phase the rate of change in composition is a balance of diffusive mass transfer to and from the NAPL body and the rate of removal of dissolved TCM by the groundwater flowing through the source zone.

$$V_w\frac{dC_w}{dt} = k_w(S - C_w) - QC_w, \tag{23}$$

where Q is the water flow rate through the source zone. Equations (22) and (23) can be solved numerically to give a

value for the time necessary for depletion of the free phase NAPL. As might be expected the time necessary for depletion is critically dependent upon the lumped mass transfer parameter, k_w. Using the previously defined data for the TCM source zone and a k_w value of 0.001 m^3 day^{-1} (a flux rate of 8.09 g day^{-1} from the residually trapped TCM to water) leads to a NAPL depletion time of 47.8 years and 62.4 years for the outflow concentration to reach a safe level. These values are much larger than those results that were obtained assuming equilibrium conditions.

It should be stressed that in general we do not have any prior knowledge of the values of the lumped mass transfer coefficients. Instead, their values are determined through fitting experimental data to a mathematical model of the system.

The mathematical model presented in Eqs. (22) and (23) can be made more realistic if we consider other sub-surface components that will absorb/adsorb organic molecules and which, as a result, will have an impact upon the length of time the source zone persists. For example, natural organic matter (NOM) is derived from the action of bacteria on biopolymers and the resulting bacterial cell debris is found on the surfaces of soils, sediments and rocks. Thermally altered NOM [30] such as coal and kerogen (the precursor of petroleum and natural gas) may also be present in the subsurface environment.

We can demonstrate quite easily that the presence of NOM increases the longevity of risk arising from water emerging from the source zone. We can use the following model which assumes that NAPL is no longer present in the source zone. However, TCM is still present: either dissolved in groundwater or ad/absorbed into NOM present in the source zone. The distribution of TCM between the aqueous and NOM phases is described by a partition constant, K_d, which can be estimated using the following equation [18]:

$$K_d = 0.41 \times f_{oc} \times K_{ow}, \tag{24}$$

where K_{ow} is the octanol water partition coefficient and whose values are widely tabulated in environmental, pharmaceutical and toxicological datasets; f_{oc} is the fraction of organic carbon present in the sample.

The equations describing the removal of dissolved TCM from the source zone are:

$$V_w \frac{dC_w}{dt} = -QC_w + k_w\left(\frac{C_{om}}{K_d} - C_w\right) \tag{25}$$

$$V_{om} \frac{dC_{om}}{dt} = k_w\left(C_w - \frac{C_{om}}{K_d}\right), \tag{26}$$

where C_{om} is the concentration of TCM in NOM and V_{om} is the volume of NOM present in the source zone. In both equations it is assumed that the NOM environment behaves as a continuously stirred reactor and as such the concentration of TCM is homogeneous throughout the phase. Equation (25) therefore describes the changing concentration of TCM dissolved in the source zone as the sum of TCM removed by water flow through the source zone $-QC_w$, TCM that transfers from the water phase to the NOM phase $-k_wC_w$ and TCM that is transferred from the NOM phase to bulk water $k_w\frac{C_{om}}{K_d}$ where the term $\frac{C_{om}}{K_d}$ is the aqueous concentration of TCM at the water/NOM interface. The terms on the right-hand side of Eq. (26) can be understood in the same way. The signs indicate the direction of transfer: the positive sign signifies transfer in and the negative sign signifies transfer out of the phase.

We assume that the initial aqueous concentration of TCM is 200 mg dm^{-3} (note for this calculation it is assumed that no NAPL is present), f_{oc} is 5% of the source zone and V_{om} is thus 0.015 m^3. We shall also assume that the presence of NOM has no impact upon water flow. K_{ow} for chloroform is $10^{1.97}$. Using these values we can solve Eqs. (25) and (26) numerically. We calculate that it takes 1100 days for the TCM in the outflow concentration to fall below a safe concentration level if NOM is absent and 1210 days if 5% NOM is present. As might be expected if the amount of NOM increases then the time for the source zone concentration to fall below a safe level becomes greater. For example, if the fraction of NOM were 10% then the time to needed for the concentration to fall below a safe level would rise to 1375 days.

These simple calculations are corroborated by many field observations that have noted that the presence of NOM prolongs the time it takes for the contaminant concentration in the plume to fall to a safe level [31].

Finally, to circumvent any confusion, it is emphasised these values are lower than those calculated earlier because no TCM is present as a separate phase. It is only present as VOC dissolved in the aqueous phase and sorbed onto the organic matter phase.

Groundwater remediation

Pump and treat

One way of treating a plume is to pump out the contaminated groundwater and treat it to remove the contamination, hence the process name, "pump and treat". Typically, one or more wells are installed in a site location, which prior investigation will have shown to be suitable. Water is then abstracted, brought to the ground surface and subsequently routed to a treatment system via a holding tank. Treatment may involve the use of activated carbon or vapour stripping and will be

determined by the nature of the VOC. For example, non-volatile components are not readily removed by vapour stripping but may be easily removed by adsorption to activated carbon.

Activated carbons are manufactured from a range of heterogeneous base materials including lignite, bituminous coal, coconut shells and wood or from relatively homogeneous material such as cellulose [32]. Activated carbon particles are porous, the pore size distribution being wide. Water-based contaminants of appropriate size enter the pores and are held in situ by intermolecular forces. The tighter the pore is the greater the strength of adsorption because of the greater number of contacts between adsorbent and adsorbate. Thus, activated carbons are useful adsorbents for small molecules [32].

For air stripping, water containing VOC(s) is sprayed into a tall packed column containing a packing material made of, for example, ceramic or steel. As the contaminated water percolates down through the column, air is pumped up through the column in the counter current direction. The intimate contact between water and air readily permits the mass transfer of VOC(s) from water to air. The process works best for VOCs that have a high Henry's law constant (cf. Eq. (8)). Clean water from the treatment process can then be discharged into a nearby stream or river. In some cases it may be pumped back into the groundwater.

What are the dimensions of a contaminant plume? Mackay and Cherry [33] catalogue the size and composition of several plumes which were documented in the USA back in the 1980s. Plume lengths ranged between 500 m to 10 km. The amount of contaminated water in the documented plumes ranged between 40,000,000 m^3 down to 102,000 m^3. However, the amount of NAPL giving rise to the plumes was in some cases relatively small. For example, one plume located at a trainyard/airport site in Denver, Colorado, was estimated to contain 80 L of dissolved NAPL components (trichloroethene, 1,1,1-trichloroethane and 1,2-dibromo-3-chloropropane) but occupied 4.5×10^9 m^3 of groundwater.

A rate constant for contaminated groundwater removal from this plume can be calculated if we use a suitable water abstraction term. A pump and treat system installed at a superfund site in Massachusetts, USA, pumped out slightly under 700 m^3 of water a day [34]. So, if this pumping rate were applied to the Denver site then the first-order rate constant for removal would be:

$$\frac{700\ (\mathrm{m^3\ d^{-1}})}{4,500,000,000\ (\mathrm{m^3})} = 1.56 \times 10^{-7}\ (\mathrm{d^{-1}}).$$

The rate constant as noted before signifies the fraction of the contaminant plume that is extracted and treated per day. The value in this case indicates that treatment will take a long time. The contaminant(s) concentration in the plume, however, are not uniform and thus not all the plume needs treatment because the contaminant concentration will be below a risk-based threshold concentration in locations further away from the source zone. Yet, supposing we only need to treat one hundredth of the plume volume and that the concentration of VOC in the vicinity of the extraction wells is 50 μg dm^{-3}, it would still take about 40 years to reduce the contaminant concentration to a safe level of 5 μg dm^{-3} [27]; this calculated value assumes that no organic matter or low permeability clay bed is present, which will increase the remediation timescales. It has therefore been concluded by many observers that pump and treat is not a particularly sustainable way of treating a plume, since the timescales involved in restoring impacted groundwater to a state that provides a minimal health risk are potentially very long [33]. It can however prove useful for hydraulically containing a contaminant plume. Pumping results in drawdown of the water table to create a cone of depression; see Fig. 7. As shown in the cartoon the formation of the cone of depression results in a steepening change in the hydraulic gradient as we get closer to the extraction well. This actually leads to a reversal of the hydraulic gradient on the down-stream side of the groundwater flow.

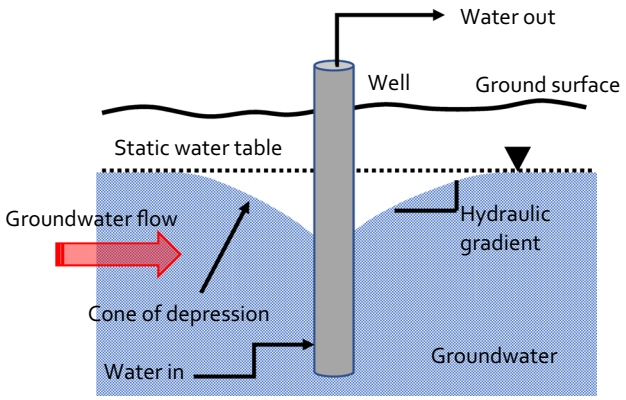

Fig. 7 Cartoon demonstrating, in elevation view, the formation of a cone of depression in the vicinity of a well. The "upside-down" triangle represents the position of the water table—the position where water pressure is equal to atmospheric pressure

If the treated groundwater has a minimal VOC concentration after treatment then it can be directly pumped back into the sub-surface where it will actually raise the water table in the vicinity of the injection well (a reversal of the cone of depression). A suitable spatial combination of extraction and injection wells can be designed to manipulate the hydraulic gradient in such a fashion that the plume is hydraulically contained as shown in Fig. 8. This is very often undertaken to protect a public water-supply borehole from a migrating contaminant plume.

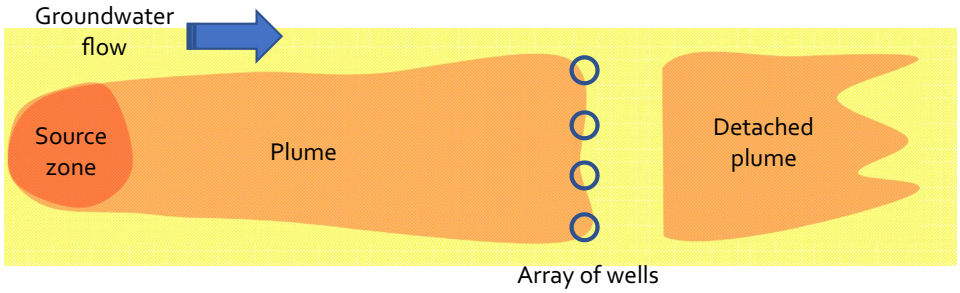

Fig. 8 Cartoon depicting in plan view hydraulic containment of a contaminant plume. Note the formation of a detached plume that is cut off from the main plume body by the working of the array of wells [1]

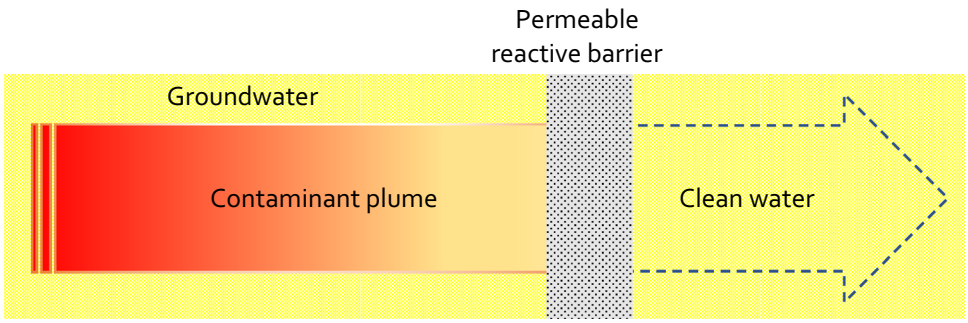

Fig. 9 Cartoon showing the functioning of a permeable reactive barrier in plan view

Permeable reactive barriers

An alternative to pump and treat, which was first proposed in the 1990s, is the use of permeable reactive barriers (PRBs). This remedial system involves the emplacement of a reactive material—that degrades the plume contaminant(s)—in an excavated sub-surface trench orientated perpendicularly to the plume. Groundwater passes through the system under natural flow conditions. The essentials of the technique are shown in the cartoon shown in Fig. 9.

The practicability of the technique was first established by Gillham and O'Hannesin [35], when they used iron metal (very often described as zero-valent iron—ZVI) to degrade chlorinated hydrocarbon compounds dissolved in water. Iron is a fairly mild reducing agent:

$$Fe^{2+} + 2e^- \underset{ox}{\overset{red}{\rightleftharpoons}} Fe^0 \quad E^o = -0.44\ V,$$

but it can readily reduce chlorinated hydrocarbons, which have reduction potentials between +0.5 and +1.5 V [36, 37], via the following reaction sequence [35]:

$$2Fe^0 \rightarrow 2Fe^{2+} + 4e^-$$
$$3H_2O \rightleftharpoons 3H^+ + 3OH^-$$
$$2H^+ + 2e^- \rightleftharpoons H_{2(g)}$$
$$R\text{-}Cl + 2e^- + H^+ \rightleftharpoons R\text{-}H + Cl^-.$$

The reaction is an example of dissolving metal reduction [37].

A VOC like trichloroethene (TCE), which is a common groundwater contaminant due to its widespread use as an industrial solvent and in chemical manufacture, can undergo several consecutive hydrogenolysis reactions that are initiated by the presence of iron. This reaction sequence is displayed in the reaction scheme shown in Fig. 10 [38] and designated pathway A. The intermediate reactions involving dichloroethenes and vinyl chloride are kinetically slow [38]. The parallel pathway results in the β elimination of chlorine and the rapid formation chloroethyne. This is followed by hydrogenolysis to ethyne and subsequent hydrogenation to ethene and ethane. Most of the TCE is degraded by β elimination [39]; only some 5–10% of the original TCE may appear as dichloroethenes (the *cis* isomer being the predominant) and vinyl chloride [38]. Since vinyl chloride is actually more toxic than TCE it is critical that the design of the system ensures that VOC residence time is sufficient to secure degradation to safe end products.

Technical and cost constraints restrict the construction of PRBs to near surface locations—the maximum depth lies between 30 and 40 m below ground surface [40]. They can therefore only be used to treat shallow, near surface, contaminant plumes. The hydraulic conductivity of the PRB should be greater than that of the surrounding aquifer material to ensure that water passively enters the system without any external stimulus. If the permeability of the PRB were lower than the surrounding aquifer material, then groundwater would tend to migrate around the PRB, following the flow pathway of least resistance.

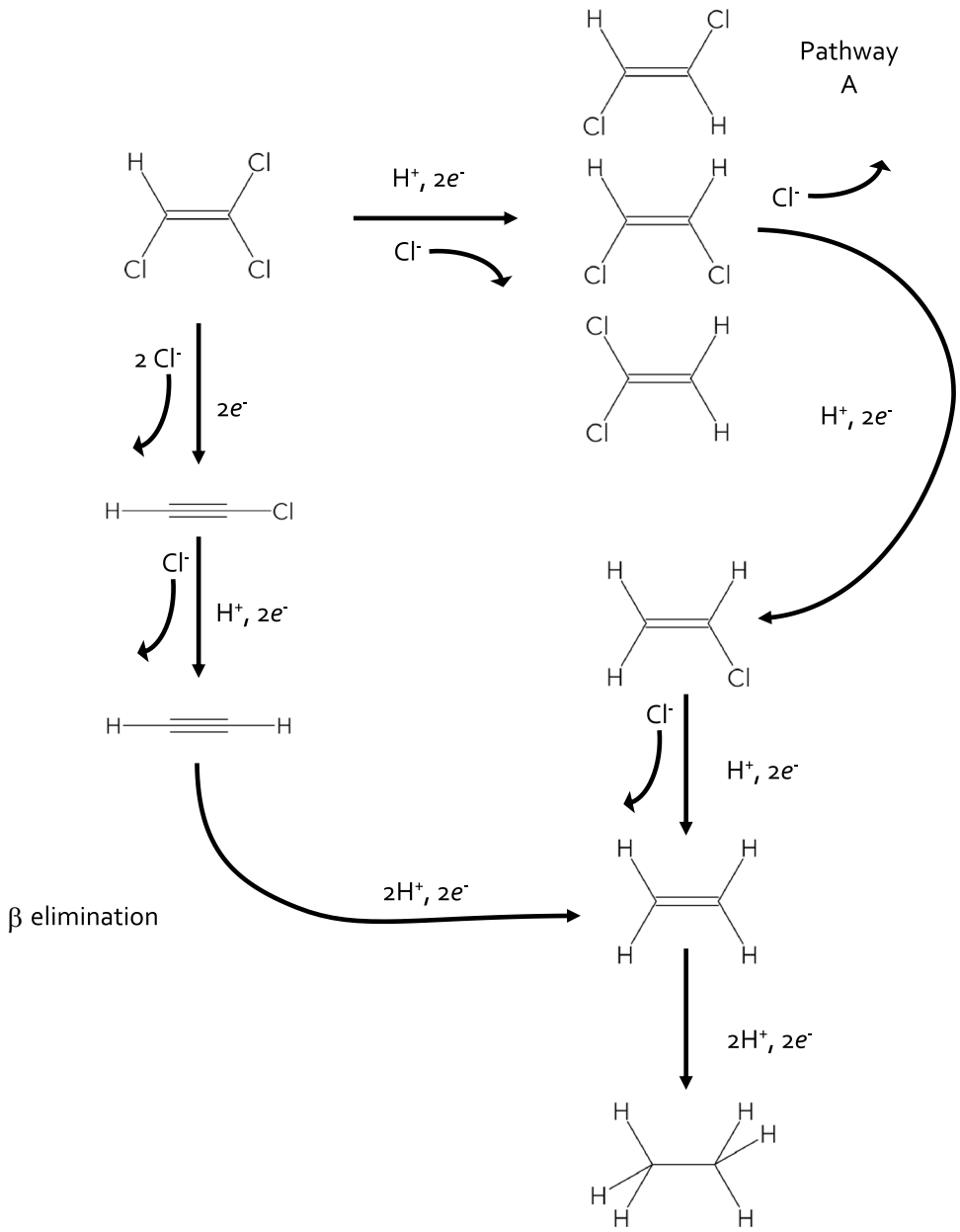

Fig. 10 Reaction scheme for the iron facilitated reduction of trichloroethene

Iron reactivity is a function of specific surface area (i.e. surface area per unit mass) and specific surface area is inversely related to particle size. Thus, fast reaction rates are obtainable using small particles. However, small particles have low permeabilities. Therefore, the chosen particle size is a trade-off between reactivity and hydraulic performance [41]. Iron grain size is usually in the range of 0.25–2.0 mm and the surface area is 0.5–1.5 $m^2\ g^{-1}$ [41]. Mixing the iron with coarse sand can also help achieve the desired PRB permeability.

The iron used in the PRB does not have to be of any particular purity. In most field applications scrap iron is used—pure iron is not necessary. In fact evidence suggests that carbon, a common impurity in iron, provides sorption sites for chlorinated organic VOCs, which actually assists in the degradation process [42].

Iron will, of course, also react with oxygen via the following reaction sequence:

$$4Fe^0 \rightarrow 4Fe^{2+} + 8e^-$$
$$8e^- + 8H^+ + 2O_2 \rightarrow 4H_2O$$
$$4Fe^{2+} + 4H^+ + O_2 \rightarrow 4Fe^{3+} + 2H_2O$$
$$4Fe^{3+} + 12OH^- \rightarrow 4Fe(OH)_3$$
$$12H_2O \rightarrow 12H^+ + 12OH^-$$

$$4Fe^0 + 3O_2 + 6H_2O \rightarrow 4Fe(OH)_3.$$

The precipitation of iron(III) hydroxide in PRB pore space can impact the permeability of the system and its precipitation on iron surfaces can impact reactivity. Long-term studies have shown that the hydraulic properties of PRBs are not adversely affected by precipitation [43]. Similarly, the surface precipitates do not seem to passivate the iron surface [38]. Problems with iron hydroxide precipitation can be obviated by installing a pre-treatment zone consisting of sand mixed with 10–15% iron. Water flowing out of this zone is deoxygenated and therefore has little impact upon iron present in the treatment zone [44].

The reaction rates can be enhanced in several ways. Matheson and Tratnyek [37] provided evidence that the rate of degradation of chlorinated methanes is inversely related to pH—at low pH values the rate of degradation is fast. The reaction of iron with oxygen clearly raises the pH of the system since it removes protons and releases hydroxide ions. Thus, it would be expected that the increase in pH should lead to a reduction in the rate of reaction. The pH of the system however may be buffered at around 7–8 by the dissolution of naturally occurring aluminosilicate minerals such as kaolinite and this enhances the rates of iron corrosion and release of protons [38, 45]. Several researchers have also examined the use of bimetallic couples—prepared by plating a second metal such as copper or nickel on iron—which accelerate the degradation of chlorinated VOCs [38].

PRBs may have one of several designs. The simplest consists of an excavated trench that perpendicularly intersects the contaminant plume, which is then back-filled with sand and granular iron. In some cases the contaminant plume is guided through the PRB by an engineered low-permeability construction (the black block in Fig. 11). Such a low permeability system can be made from clay, which has a low hydraulic conductivity, metal sheet pilings or even a hydrophobic textile that is impermeable to water. The low permeability unit forms a funnel, and the funnel exit comprises the PRB. Such a system is referred to as a funnel and gate.

In situ chemical oxidation (ISCO)

Despite the success of PRBs to deal with some plumes it is not necessarily the answer for all contaminant plumes. PRBs are useful for degrading chlorinated organic VOCs and for reducing plumes containing chromium (which is not a focus of this lecture text). However, plumes created by the release of aliphatic and aromatic hydrocarbon NAPLs are not affected by reductants like iron since they are already in their most reduced state. Moreover, treatment of plumes located deep below ground surface, using PRB technology, would provide enormous technical and cost challenges. This has led some researchers to examine the use of alternative techniques for the remediation of VOC plumes. One remedial intervention that has been investigated, and which has shown some success, is the injection of an oxidant solution into the plume. Several oxidant systems have been considered and tested; these include: (1) potassium and sodium permanganate [46]; (2) Fenton's reagent—a mixture of hydrogen peroxide and iron (II) ions [47]; (3) sodium persulphate [48]; (4) ozone [49]. A range of organics are treatable by ISCO. ISCO-treatable VOCs derived from common NAPLs include [50]:

- benzene, methylbenzene, ethylbenzene and dimethylbenzene—these are commonly encountered in petroleum and petroleum products;
- 2-methoxy-2-methylpropane (methyl tertiary butyl ether—MTBE)—this is a commonly used additive in petrol to improve its anti-knock properties;
- petroleum hydrocarbons;
- chlorinated hydrocarbon solvents;
- polyaromatic hydrocarbons—these are often encountered in coal tar and creosote;
- polychlorinated biphenyls—these compounds were widely used, as oils, in electrical equipment such as capacitors and transformers and as heat transfer agents. Because of their toxicity their use has been phased out but because they are extremely stable they are still

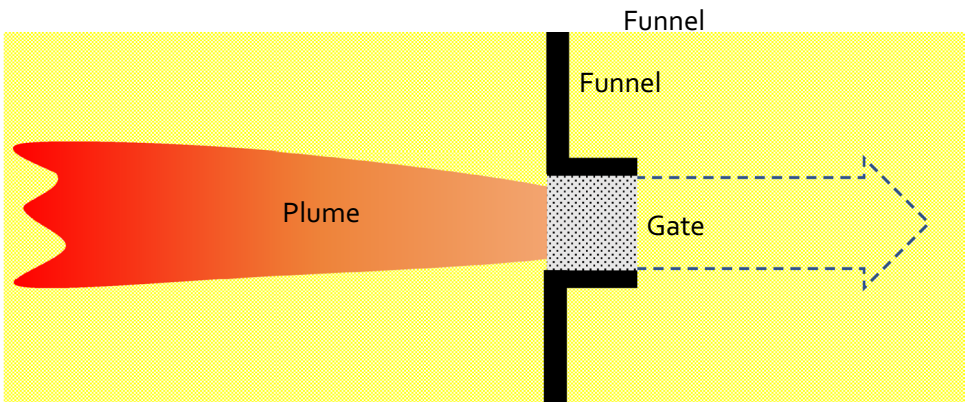

Fig. 11 Cartoon of a funnel and gate system in plan view

encountered in electrical equipment and in the environment.

We shall look at two systems: permanganate oxidations and iron-catalysed hydrogen peroxide decompositions.

Permanganate oxidation

Permanganate oxidations are carried out using either potassium or sodium permanganate. Solutions of potassium permanganate are commonly made up on site. The solubility of potassium permanganate is limited and the highest achievable concentrations are around 20–40 g dm^{-3} [47]. Sodium permanganate is normally supplied as a concentrated, 40%, solution. The counter ion makes little difference to reactivity. However, the rates of reaction are dependent upon permanganate concentration.

There are always potential problems associated with using a strong oxidant in powder form so the use of sodium permanganate in solution may be preferred on-site. However, the higher achievable aqueous concentrations using sodium permanganate may create a highly exothermic reaction if brought into contact with high reductant concentrations in groundwater.

Permanganate is used to oxidize compounds with double bonds such as alkenes, aldehydes and ketones. It readily interacts with π bonds [51]. It is not, however, able to oxidize commonly encountered aromatic compounds like benzene where the delocalised π electrons are more tightly bound. Permanganate is also not effective against saturated organic compounds.

In the pH range 3.5–12, which encompasses the normal pH values encountered in groundwater, permanganate undergoes a three-electron reduction via the following reaction mechanism [50]:

$$MnO_4^- + 2H_2O + 3e^- \rightarrow MnO_2(s) + 4OH^-.$$

The reactions with chlorinated ethenes are outlined below [50]:

Tetrachloroethene

$$4KMnO_4 + 3C_2Cl_4 + 4H_2O \rightarrow 6CO_2 + 4MnO_2(s) + 4K^+ + 12Cl^- + 8H^+$$

Trichloroethene

$$2KMnO_4 + C_2HCl_3 \rightarrow 2CO_2 + 2MnO_2(s) + 2K^+ + 3Cl^- + H^+$$

Dichloroethene

$$8KMnO_4 + 3C_2H_2Cl_2 + 2H^+ \rightarrow 6CO_2 + 8MnO_2(s) + 8K^+ + 6Cl^- + 4H_2O$$

Chloroethene

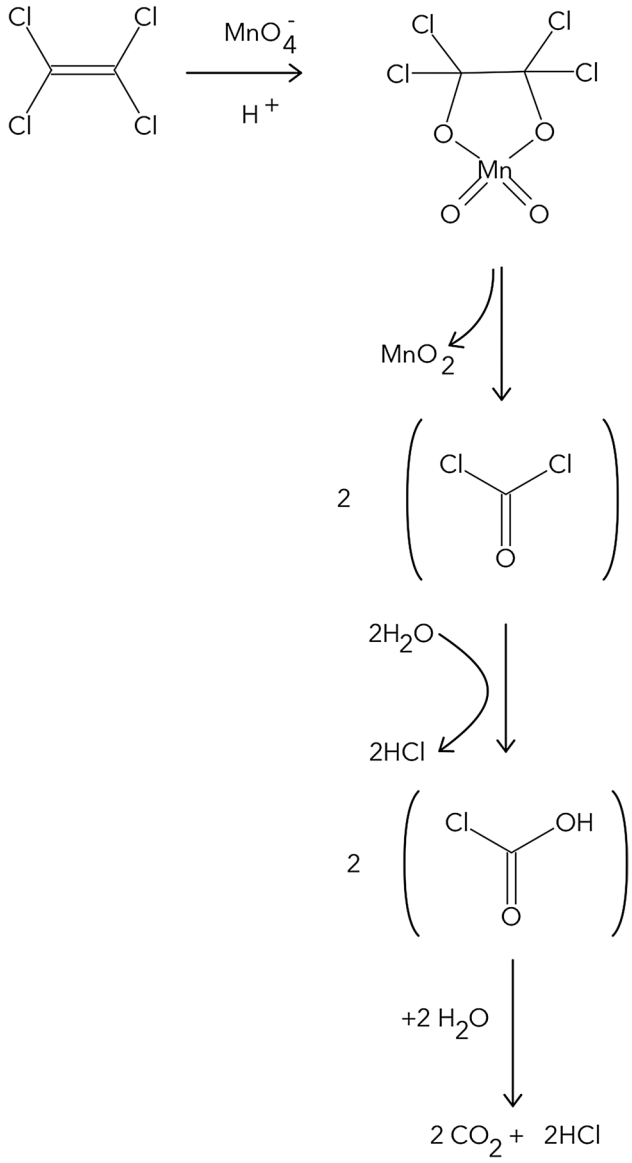

Fig. 12 Permanganate oxidation of tetrachloroethene at low pH

$$10KMnO_4 + 3C_2H_3Cl \rightarrow 6CO_2 + 10MnO_2(s) + 10K^+ + 3Cl^- + 7OH^- + H_2O$$

These reactions are second order [52, 53] with respect to the chlorinated ethene substrate and permanganate. Laboratory studies have further confirmed that chlorinated ethenes are completely degraded to harmless end products [53].

A reaction mechanism for the degradation of tetrachloroethene at low pH is shown in Fig. 12 [52]. Degradation reaction rates are affected by the presence of competing organic substrates such as NOM [50]. Degradation of NOM could be fortuitous—VOCs are ad/absorbed by NOM and its destruction will result in their release to groundwater where

they can then react with permanganate. However, treatability studies will be necessary prior to field-scale injection to establish the concentration of permanganate needed to ensure the complete destruction of the chlorinated ethene VOC. One advantageous aspect of permanganate's chemistry is that it is fairly stable in the sub-surface and as a result is persistent [50].

A common feature of all the reactions shown above is the formation of solid manganese (IV) oxide particles. This can be a problem for the degradation of chlorinated ethene VOCs encountered, for example, in low-permeability zones [54], since capture of particles at pore throats or their accumulation in pores can severely reduce the permeability of the zone which in turn can result in the isolation of the VOC plume from further interaction with permanganate [55]. Laboratory studies, however, have shown that the co-injection of sodium hexametaphosphate (SHMP) with permanganate can inhibit the aggregation of manganese (IV) oxide particles to form a precipitate resulting in a better VOC degradation outcome [54]. It would appear that SHMP stabilized particles (particle sizes are ≤ 0.1 μm) are protected against agglomeration through electrostatic repulsion [55]; the zeta potential of the particles stabilized by SHMP being about − 26 mV [55]. Such small particles are readily retained in flowing groundwater and the negative zeta potential should prevent adsorption to the negatively charged sub-surface mineral surfaces.

Unfortunately, SHMP may also disperse clays like kaolinite [56], which may have the effect of reducing the permeability of fine grained porous media as mobile clay particles are trapped at pore throats.

In general, permanganate is used to degrade VOCs dissolved in groundwater. However, there has been at least one study where permanganate has been used to treat both a tetrachloroethene and a mixed trichloroethene/tetrachloroethene DNAPL source zone [46]. Essentially, permanganate was formulated as a 10 g dm^{-3} solution and was flushed through the source zone at the rate of 50 dm^3 day^{-1}. For the mixed DNAPL, 8 dm^3 was emplaced into a test cell located in a site in Borden, Ontario. After flushing for 290 days there was a 62% reduction in the amount of DNAPL.

Fenton's reagent

Hydrogen peroxide is an oxidant that can be used in ISCO. However, the kinetics of VOC degradation by hydrogen peroxide alone is too slow. The addition of a solutions of Fe(II) ions rapidly increases the rate of reaction. The mixture of hydrogen peroxide and iron (II) ions, which is often referred to as Fenton's reagent—acknowledging the first chemist who described the use of this system—decomposes in the following way:

$$H_2O_2 + Fe^{2+} \rightarrow OH\cdot + OH^- + Fe^{3+}.$$

OH· is the oxidant of interest. If the pH of the system is kept < 5 then the Fe(III) is reconverted back to Fe(II) and thus remains in solution to help catalyse further breakdown of hydrogen peroxide [50]. The system originally used by Fenton consisted of a dilute solution of hydrogen peroxide and Fe(II) ions [57]. It is, however, extremely difficult to maintain a well-mixed low concentration of peroxide in groundwater; thus, a modified Fenton's system is used [50], which involves the injection of a 4–20% solution of hydrogen peroxide and co-injection of Fe(II) in acid solution into the VOC plume in groundwater. The acid used may be hydrochloric, sulphuric or ethanoic acid.

The OH· radical can undergo electrophilic substitution with aromatic compounds [58] and addition reactions with alkenes [59]. In addition, the hydroxyl radical can abstract hydrogen atoms from saturated compounds like alkanes [47]. The reactions are kinetically second order and are fast—in some cases the limit on the rate of reaction arises solely from the diffusion of the reactants. A diffusion limited rate constant is of the order of 10^{10} M^{-1} s^{-1} [59]. A study of the kinetics of the reaction between hydroxyl radicals and substituted benzenes showed that the rate constants is > 10^9 M^{-1} s^{-1}, and it is considered that rate constants which are > 10^9 M^{-1} s^{-1} are suitable for ISCO [47].

Apart for the hydroxyl radical, other species are formed when the concentration of hydrogen peroxide is high. These radical species are obtained by the reaction of hydroxyl radicals with hydrogen peroxide.

The hydroperoxyl radical, $HO_2\cdot$, is formed in the following way:

$$OH\cdot + H_2O_2 \rightarrow HO_2\cdot + H_2O \quad k = 2.7 \times 10^7\ M^{-1}\ s^{-1},$$

the superoxide radical anion is formed by proton dissociation:

$$HO_2\cdot \rightleftharpoons O_2^-\cdot + H^+ \quad pK_a = 4.8,$$

and the hydroperoxide anion is formed via the following reaction:

$$HO_2\cdot + Fe^{2+} \rightarrow HO_2^- + Fe^{3+} \quad k = 1.2 \times 10^6\ M^{-1}\ s^{-1}.$$

Radical species, R·, emerging from the interactions of hydroxyl radicals with the VOCs, can be important in the formation of more hydroxyl radicals:

$$R\cdot + H_2O_2 \rightarrow ROH + OH\cdot$$

The rate constant for the formation of the hydroperoxyl is quite low but for systems where the concentration of hydrogen peroxide is high the concentrations of hydroperoxyl

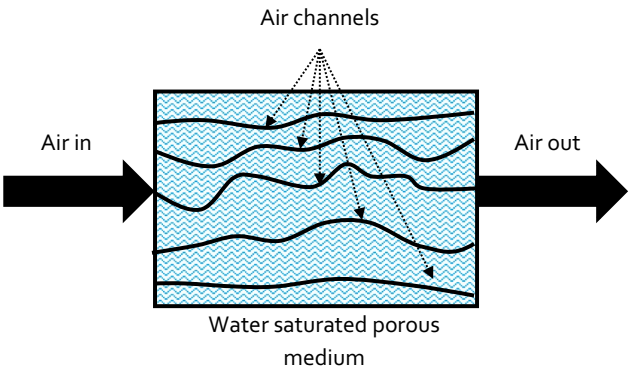

Fig. 13 Cartoon depiction of air sparging

superoxide radicals and the hydroperoxide anion become significant [47].

The presence of these species aids the degradation of a whole variety of VOCs making it a near universal treatment system [47]. Indeed, modified Fenton's reagent can be further used to degrade VOCs that are sorbed to NOM and treat NAPL source zones.

Air sparging and vapour extraction

Air sparging and vapour extraction are used as remedial technologies in field situations where the NAPL components present in the sub-surface are readily removed via the vapour phase. Air sparging involves the injection of air below the water table followed by the subsequent partitioning from the water phase to the vapour phase of organic components. Vapour extraction involves the pumping out of air from the unsaturated zone which contains volatile organic compounds that have already partitioned from groundwater to the air phase. Often the two technologies are used together in order that the contaminated vapour phase is removed and treated.

We can create a simple mathematical model of how air sparging works based upon the cartoon shown in Fig. 13. It is understood that as the injected air passes through groundwater it forms air channels [60] that are in direct contact with groundwater, shown in Fig. 13. The air channels will, depending upon air pressure and the capillary forces generated at the pore throats (see Ref. [2]), occupy a relatively small fraction of the porous medium.

The change in the mass of the volatile organic compound (VOC) in the aqueous phase with time (t, dimension T) is given by the following equation:

$$V_w \frac{dC_w}{dt} = -QC_a, \tag{27}$$

where C_w and C_a are the concentrations of VOC in water and air respectively (ML^{-3}), V_w is the volume of water (L^3) and Q is the volumetric throughput of air ($L^3\,T^{-1}$). Equation (27) arises from the assumption that as the VOC is removed by the injected air flow more VOC will immediately partition into the air phase from the aqueous phase. The amount that partitions is determined by the aqueous phase concentration and the partition coefficient K_{aw}.

Equation (27) can then be used with Eq. (8) to give:

$$V_w \frac{dC_w}{dt} = QK_{aw}C_w. \tag{28}$$

Integration of Eq. (28) gives the following first-order kinetic expression:

$$C_w = C_0 e^{-\frac{QK_{aw}}{V_w}t}, \tag{29}$$

C_0 is the aqueous phase concentration of the VOC at time zero. The exponent term QK_{aw}/V_w has the dimensions of (T^{-1}) which of course makes this a first rate constant. The rate constant essentially describes the fraction of material that is removed per unit time.

The graph in Fig. 14 shows the reduction in the aqueous concentration of VOC with time for a model system and clearly shows that the magnitude of the value of K_{aw} determines the length of time it takes for the removal of the VOC. The greater the value of K_{aw} is the smaller the time interval necessary for VOC removal to an environmentally safe endpoint. If for example a safe limit for the concentration of VOC in water is 10^{-6} g dm^{-3} then for $K_{aw}=1$ the time necessary to reduce the aqueous concentration to this level is 46 h. If $K_{aw}=0.01$ the time necessary to achieve this level is two orders of magnitude greater at 4605 h.

Equally, the greater the value of Q is the less time necessary for reduction in aqueous concentration to below a safe

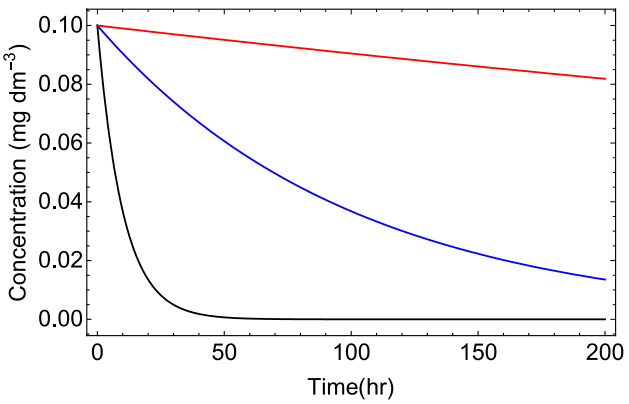

Fig. 14 Graph showing how the concentration of VOC in the aqueous phase varies with time for K_{aw} values of 0.01, 0.1 and 1. V_w is set equal to 1 m^3 and Q is set to 0.1 $m^3\,h^{-1}$. The initial VOC concentration C_0 is set equal to 0.1 mg dm^{-3}

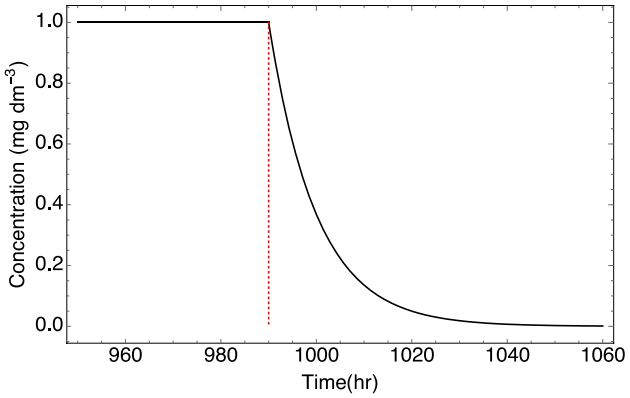

Fig. 15 Reduction in VOC concentration when NAPL is present. The parameters are the same as those in Fig. 14. K_{aw} is 1 and the amount of NAPL present is 100 mg. VOC solubility is 1 mg dm^{-3}

level. If the safe level is again 10^{-6} g dm^{-3} and $K_{aw}=1$ then at $Q=0.2$ m^3 h^{-1} the time necessary to achieve the safe level is 23 h and for $Q=0.3$ m^3 h^{-1} the time necessary is 15.4 h. These numbers bear no resemblance to what we might encounter in the field, but they do provide an indication of how the various parameters associated with air sparging affect the final results.

If NAPL is present in the sub-surface volume then, for a system that we assume to be at equilibrium, the aqueous phase will be saturated with VOC. Air sparging will reduce the NAPL mass but the aqueous phase concentration will remain constant. Once the NAPL is depleted and no longer exists as a separate liquid phase, the VOC concentration will be reduced, as shown in Fig. 15.

The time necessary to deplete the NAPL as a separate liquid phase is given by solution of the following expression:

$$\frac{M_0 - S K_{aw} Q t_d}{V_w} = S. \tag{30}$$

M_0 is the original mass of NAPL (M), S is the solubility of the NAPL in water (we assume that the NAPL contains a single component) (ML^{-3}), Q is the air flow rate (L^3 T^{-1}), V_w is the volume of water and t_d is the time to depletion. The term $S K_{aw} Q t_d$ merely represents the total amount of VOC removed by the air phase in time t_d. SK_{aw} converts the aqueous phase concentration into an vapour phase concentration. $SK_{aw}Q$ converts the air concentration into the amount of VOC removed per unit time. $SK_{aw}Qt_d$ calculates the total amount of VOC removed over time, t_d. This term is then subtracted from M_0 and divided by V_w to give an apparent aqueous phase concentration. If this apparent concentration is greater than the aqueous solubility of the VOC then NAPL must still be present. Once the apparent concentration is equal to the solubility the VOC ceases to exist as a separate liquid phase. For the system shown in Fig. 3 it takes about 41.3 days to deplete the NAPL. If the value of K_{aw} is an order of magnitude lower then it would take something like 1.13 years to remove the NAPL. Moreover, we would still need to carry on sparging to reduce the aqueous phase concentration to a safe level.

The treatment so far has been based upon the assumption that the relationship between the concentrations of VOC in the vapour and aqueous phases is related by the modified Henry's Law Constant K_{aw}. This assumption clearly implies that the VOC can migrate across the interface at such a rate so as to continuously and instantaneously maintain thermodynamic equilibrium. However, the existence of boundary layers on both the water side and vapour side, where the respective fluids are stagnant, provides a resistance to mass transfer across the interface. These boundary layers arise even if both fluids are turbulent because eddies created by turbulence are damped at the interface [18]. A conceptual model for mass transfer in the air/water system drawn from Ref. [18] is shown in Fig. 16. We can use the diagram as the basis for producing a lumped parameter model for air sparging.

The VOC flux J (M T^{-1}) on the water side is given by:

$$J = k_w A(C_w - C_{w,i}), \tag{31}$$

where k_w is the water side mass transfer coefficient (L T^{-1}), A is interfacial area (L^2) and C is concentration (ML^{-3}). The subscripts w and i refer to water and interface respectively. The equation is written such that that flux goes from high concentration (the bulk water concentration—C_w) to low concentration (the VOC concentration at the interface—$C_{w,i}$—is lower).

A similar expression can be given for VOC flux on the air side:

$$J = k_a A(C_{a,i} - C_a), \tag{32}$$

where the subscript a refers to air.

We assume that the bulk phases are well-mixed reactors so that the bulk phase concentrations are homogeneous throughout the respective bulk phases. We assume that the concentrations at the interface are in thermodynamic equilibrium. Thus:

$$\frac{C_{a,i}}{C_{w,i}} = K_{aw}. \tag{33}$$

We do not make this assumption about the bulk phase concentrations.

We can rewrite Eq. (32) as:

$$C_{a,i} - C_a = \frac{J}{k_a A}. \tag{34}$$

Similarly we can rewrite Eq. (31) and substitute for $K_{w,i}$ using Eq. (33) to give:

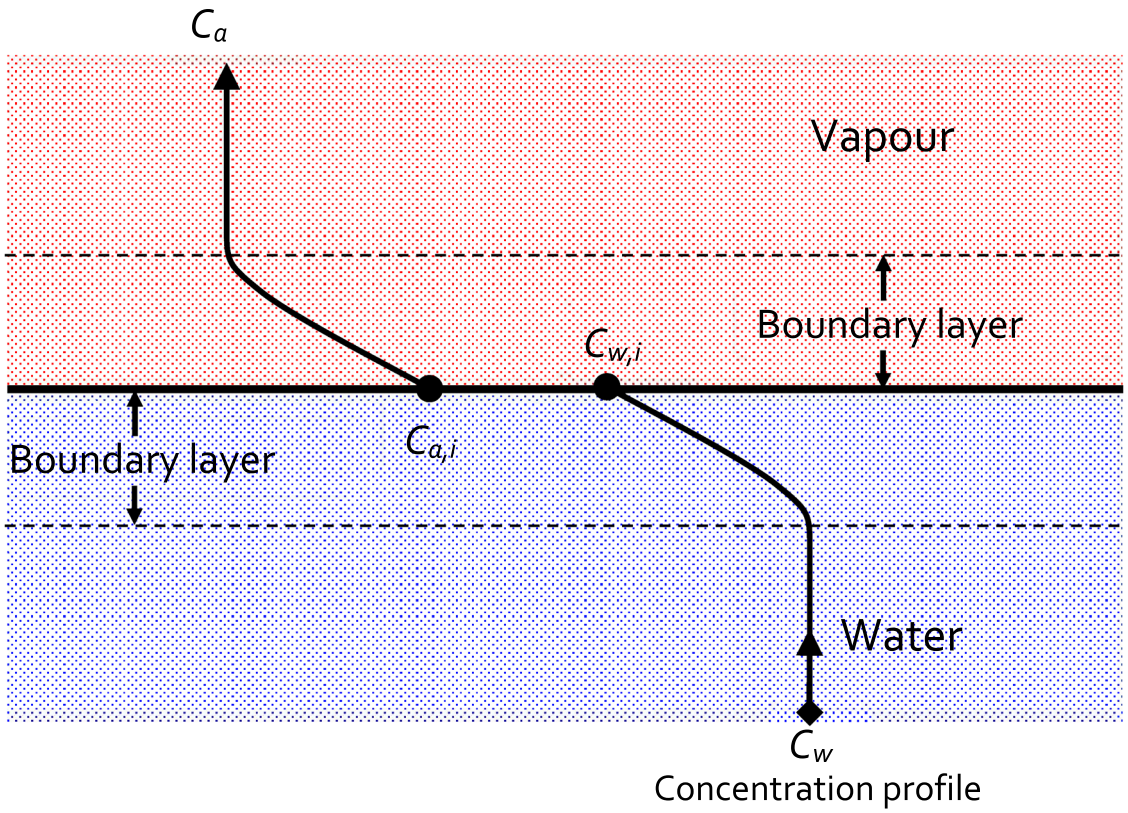

Fig. 16 Conceptual model of mass transfer between the water and vapour phases. The concentration profile graphically depicts how VOC concentration changes going across the interface. In particular, the graphic shows that $C_w > C_{w,i}$ and $C_{a,i} > C_a$

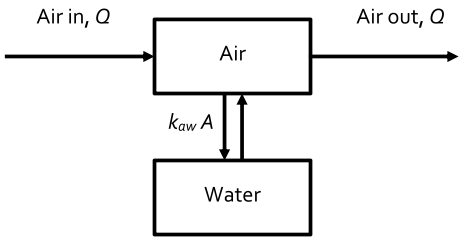

Fig. 17 Conceptual model of air sparging used to create Eqs. (39) and (40)

$$C_w K_{aw} - C_{a,i} = \frac{JK_{aw}}{k_w A}. \tag{35}$$

If we add Eqs. (34) and (35) we obtain the following expression:

$$C_w K_{aw} - C_a = \frac{J}{A}\left(\frac{K_{aw}}{k_w} + \frac{1}{k_a}\right). \tag{36}$$

The term in brackets is usually identified as an overall mass transfer coefficient [61]:

$$\frac{1}{k_{aw}} = \frac{K_{aw}}{k_w} + \frac{1}{k_a}. \tag{37}$$

Thus, the flux equation can be written as:

$$J = k_{aw}A(C_w K_{aw} - C_a). \tag{38}$$

We use the schematic in Fig. 17, which shows the flow of material in our air sparging system, to create a lumped-parameter model to describe air sparging.

Two equations can be written for each environmental compartment. For the vapour phase we can write using Eq. (38):

$$V_a \frac{dC_a}{dt} = k_{aw}A(K_{aw}C_w - C_a) - QC_a, \tag{39}$$

and for the aqueous phase

$$V_w \frac{dC_w}{dt} = k_{aw}A(C_a - K_{aw}C_w). \tag{40}$$

Again, the mass transfer coefficient and interfacial area can be combined into a lumped-parameter with the units of

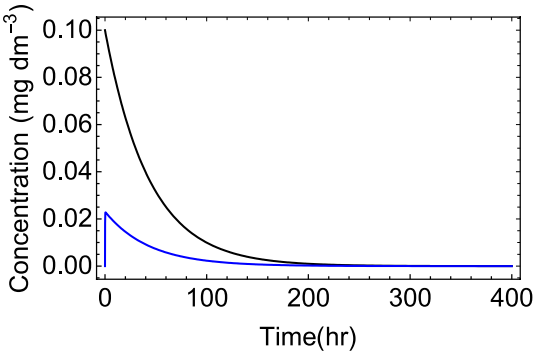

Fig. 18 Plot of VOC concentration in the aqueous and vapour phases. The plot was created by numerical solution of Eqs. (39) and (40) using the parameter values outlined in the text

$L^3\ T^{-1}$. This parameter when multiplied by concentration describes the fraction of VOC that is transferred per unit time.

Both equations are written as a rate of change in VOC concentration in either phase. On the right-hand side of each equation the various expressions represent either rates of entry into the phase or rates of departure. Rates of entry are added; rates of departure are subtracted. The mass transfer coefficient describes the rate of transport of VOC in either direction—either from the air/water interface to the air phase or the air phase to the interface.

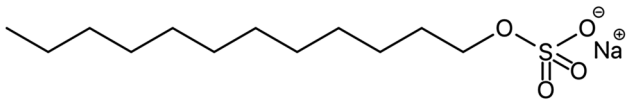

Fig. 20 Sodium dodecyl sulphate

The thermodynamic driving force for transfer is the partition coefficient. However, the removal of contaminated air ensures that VOC is ultimately transported from the aqueous phase to the air phase and subsequently removed from the system.

Equations (39) and (40) can be solved numerically to provide the plots shown in Fig. 18. The parameters used to obtain Fig. 18 are the same as before. K_{aw} is set to 1, Q is set to 0.1 $m^3\ h^{-1}$ and k_{aw} is set to 0.03 (which seems a reasonable value [62]).

Numerical solution of Eqs. (39) and (40) allows us to calculate the time necessary to reduce the aqueous phase VOC concentration to a safe level. In this particular case if the safe level is once again 10^{-6} g dm^{-3} then it will take 200 h to reach this concentration. This is nearly four times longer than the time predicted using the equilibrium model and clearly shows the need to consider mass transfer.

The models presented can be made more realistic by incorporating other processes that are likely to be encountered in real systems such as adsorption and degradation. As we saw previously [2] organic contaminants dissolved

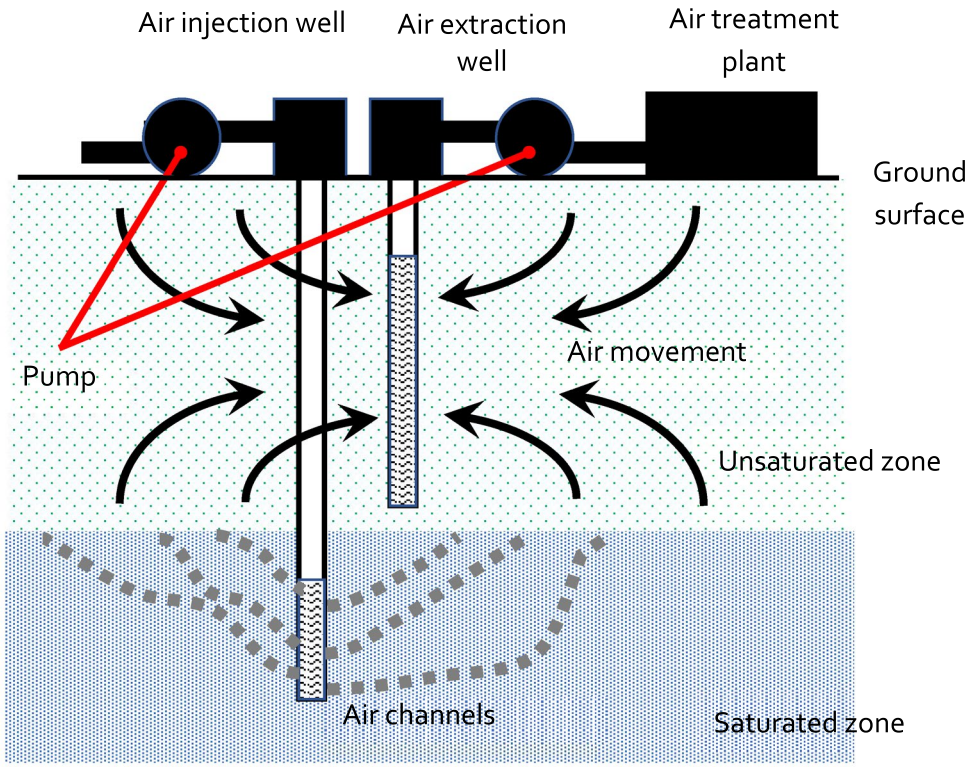

Fig. 19 Cartoon showing the field implementation of air sparging

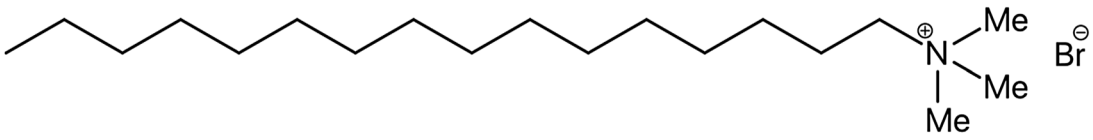

Fig. 21 Hexadecyltrimethylammonium bromide

in water are adsorbed/absorbed by organic matter attached to solid surfaces in soil and rock systems. Furthermore, it should be anticipated that for VOCs that are readily degraded by aerobic microorganisms—such as petroleum hydrocarbons—the introduction of air will augment the sub-surface oxygen levels and encourage the further biodegradation of these VOCs. This latter process is sometimes referred to as biosparging.

Figure 19 schematically shows an air sparging system. In this set-up one well is sunk down into the saturated zone—this is the zone where all pore spaces are filled with water. A second well is placed in the unsaturated zone—the zone that is variably saturated with air and water. Air is injected into the saturated zone and moves through air channels. These air channels arise because of a phenomenon known as viscous fingering. Viscous fingering is the unstable displacement of a more viscous fluid by a less viscous fluid [63].

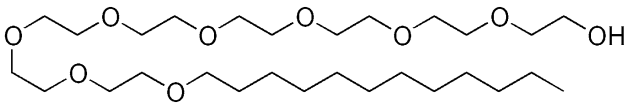

Fig. 22 Octaethylene glycol monododecyl ether

Surfactant facilitated groundwater remediation

The term surfactant is derived from the term **surf**ace **act**ive **a**ge**nt**. Surfactants are amphiphilic molecules that chemically combine non-polar hydrophobic (water repelling) and polar hydrophilic (water attracting) moieties. The non-polar fragment is normally an alkyl chain. The polar group may be either ionic—both anionic and cationic groups are encountered—or a non-ionic water soluble polar segment, which may be made from a sugar or a polyether like polyethylene oxide.

A typical anionic surfactant, sodium dodecyl sulphate, is shown in Fig. 20.

A typical cationic surfactant hexadecyltrimethylammonium bromide is shown in Fig. 21

A typical non-ionic surfactant, octaethylene glycol monododecyl ether, is shown in Fig. 22.

When added to water the differing solvent preferences of the two parts of the surfactant molecule are accommodated by two separate mechanisms, depending upon the surfactant concentration:

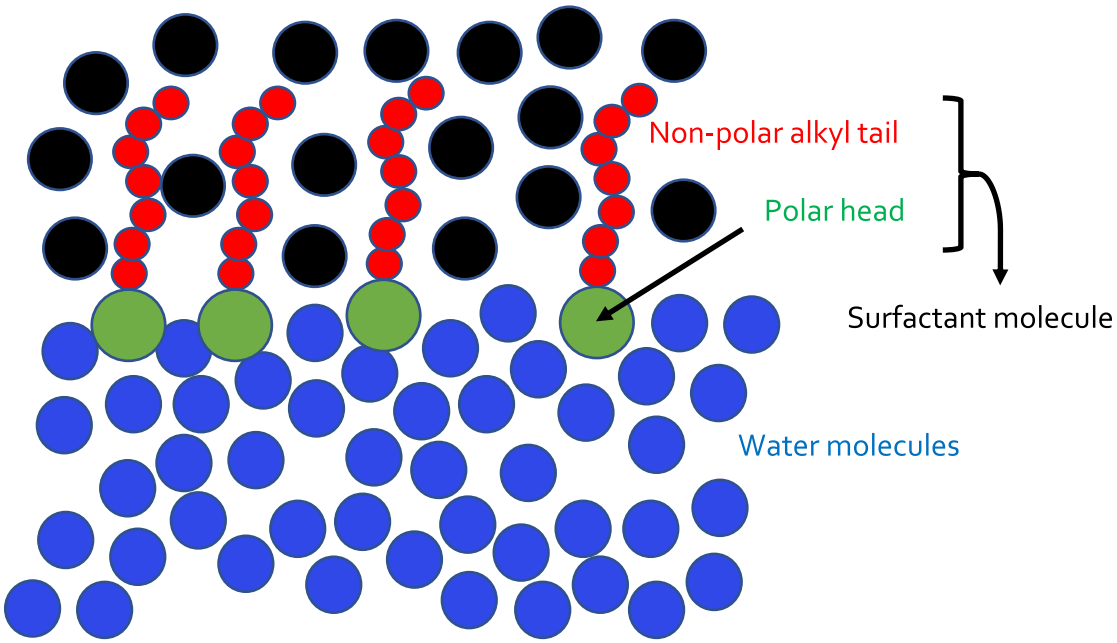

Fig. 23 Cartoon showing the adsorption of surfactant molecules at the at the interface between water (blue) and NAPL (black)

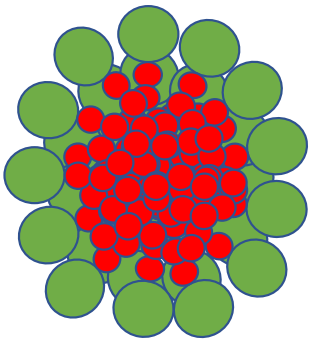

Fig. 24 Cartoon showing a section cut through a micelle. The cartoon shows an interior composed of alkyl chains surrounded by a corona of polar head groups that facilitate the easy dispersion of a micelle in water

- Surfactant adsorption at the air/water interface or at the interface between water and a NAPL (Fig. 23).
- Through micelle formation (Fig. 24) above a critical concentration.

Adsorption at the interface between water and a NAPL permits the non-polar tail of the surfactant to orientate and embed itself in the non-polar NAPL phase thereby "expressing" its phase preference. Similarly the polar head remains located in the aqueous phase. Adsorption of surfactant molecules at interface between water and a NAPL has the effect of reducing the NAPL/water interfacial tension. Several explanations can be advanced for this reduction. The immiscibility of water and a NAPL indicates that there is a free energy penalty arising from contact at an interface between the two phases. The free energy penalty arises from the breaking of hydrogen bonds between water molecules and their replacement by much weaker van der Waals forces between NAPL molecules and water. This free energy penalty gives rise to the interfacial tension. Indeed, the interfacial free energy per unit interfacial area is numerically equal to the interfacial tension [64]. The replacement of water molecules at the interface by surfactant molecules reduces this free energy penalty and thus reduces the interfacial tension. Whilst this explanation may provide a thermodynamic rationale for interfacial tension and its reduction by surfactant molecules, it does not provide a physical explanation for the emergence of the contractile force at the interface and its reduction by surfactant adsorption.

The contractile force underpinning interfacial tension arises from the non-isotropic distribution of pressure at the interface. Pressure has a kinetic and static component. The kinetic component arises from the transport of momentum across an imaginary test interface. The static component arises from the intermolecular forces acting between molecules acting across the imaginary test interface. In general, these forces are attractive and thus negative—except when the molecules are extremely close—and as such they reduce the overall pressure since they are subtracted from the kinetic component. In the bulk phases the kinetic and static components are isotropic. At the interface the static component across imaginary test surfaces drawn normally and tangentially to the interface is different. The tangential static component is greater than the normal static component (see Refs. [2, 64, 65] for an explanation) and thus the tangential pressure is lower than the normal pressure (which is equal to atmospheric pressure). This is the origin of interfacial tension.

Surfactants increase the pressure acting tangentially to the surface [66]. This surface pressure increase presumably arises from the electrostatic repulsions that develop between the ionic headgroups or from the entropic penalties that occur from the interactions between the polar head groups. These repulsive effects decrease the static pressure contribution to the tangential pressure and thus lead to a reduction in surface/interfacial tension.

The surface/interface cannot hold an unlimited amount of surfactant. There comes a point where the surface is saturated. Further addition of surfactant results in micelle formation. Micelle formation represents an alternative way through which surfactant molecules can resolve their solvent preferences. The hydrophobic tails of the surfactant molecules self-aggregate to reduce their exposure to water whilst at the same time the polar surfactant head groups remain in contact with the aqueous phase. The interior of a micelle is essentially a non-polar solvent. For example, micelles formed from sodium dodecyl sulphate have an interior that is essentially dodecane—a liquid hydrocarbon solvent. As a liquid the dodecane chains close to the sulphate head group are constrained to be more or less perpendicular to the surface; however, the rest of the chain acts as a normal liquid [67]. The micelle exterior favourably interacts with water due to the polar head groups. This permits the facile dispersion of micelles in water. Micelles are thus in effect small volumes of non-polar liquid solvents dispersed in water. The micelle depicted in Fig. 24 is spherical. However, micelles are not necessarily spherical and they may take on a number of different structures such as cylindrical or lamellar [68]. Finally, micelles are formed when the aqueous surfactant concentration is greater than a concentration threshold called the critical micelle concentration (cmc).

One important property of micelles is their ability to solubilise hydrophobic compounds. Solubilisation is the process whereby a hydrophobic organic compound (HOC) partitions from a solid or separate liquid phase to the interior of a micelle via the aqueous phase. The process increases the apparent aqueous solubility of the HOC. An example of

solubilisation is shown in Fig. 25; the data were taken from Ref. [69]. The surfactant used is a poly(ethylene oxide)-poly(propylene oxide) block copolymer with the approximate formula $(EO)_{17}$ $(PO)_{60}$ $(EO)_{17}$ and trade name P103 (the generic structure is shown in Fig. 26). The propylene oxide (PO) block is the hydrophobic moiety. The ethylene oxide (EO) blocks are hydrophilic. The plot shows that the solubility enhancement—the ratio of the apparent aqueous solubility in the surfactant solution to the pure water aqueous solubility—increases as the surfactant concentration increases above the cmc. In this example there is also some indication of an increase in apparent solubility below the cmc, which seems to be a feature of these block copolymeric surfactants [69].

Several investigators have examined the use of aqueous surfactant solutions for the removal of NAPL residues from soils. Typically, the NAPLs studied have included coal tar and petroleum hydrocarbons. Paterson et al. [70] examined the use of a range of ethylene oxide/propylene oxide block copolymers (see Fig. 26) to remove named polyaromatic hydrocarbons from a coal tar contaminated soil obtained from a former manufactured gas site located in London.

Manufactured gas or Town Gas was produced by the heating of coal in an anoxic atmosphere. The gas produced was used for domestic cooking, heating and lighting. Coal tar, a complex mixture of phenolic, polyaromatic hydrocarbon (PAH) and heterocyclic compounds, was a by-product of the process. Thus, many former manufactured gas sites are contaminated with coal tar (see for example Fig. 1).

The soil water distribution coefficient (K_d) is defined as the ratio of the concentration (C) of a compound (x) in soil (s) and water (w):

$$K_d = \frac{C_s}{C_w}. \tag{41}$$

Figure 27 shows how increasing surfactant concentration increasingly reduces the value of K_d for naphthalene, indicating that the amount of naphthalene desorbed from soil to the aqueous phase increases with increasing surfactant concentration. Moreover, at moderate surfactant concentrations K_d is reduced to quite low values suggesting that contaminant concentrations in soils can be reduced to levels that are below risk-based quality guidelines.

Surfactant facilitated contaminant desorption can be used as the basis for an engineered soil remediation system. Such a system can be designed to be either ex situ or in situ. Ex situ remediation typically involves the extraction and removal of the soil from its site location and its subsequent treatment with an aqueous surfactant solution. In situ remediation typically involves flushing an aqueous surfactant system through the contaminated subsurface location.

Most studies examining the surfactant facilitated removal of contaminants from soil are laboratory studies. However, there have been some field studies. For example, Iturbe et al. undertook the remediation of soil located in a former petroleum distribution and storage facility located in Mexico [72]. Their investigation focussed upon the removal of petroleum

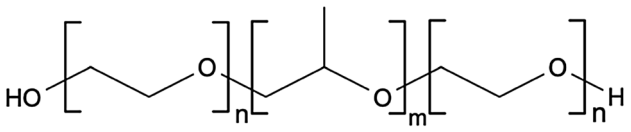

Fig. 26 Structure of an ethylene oxide/propylene oxide block copolymer

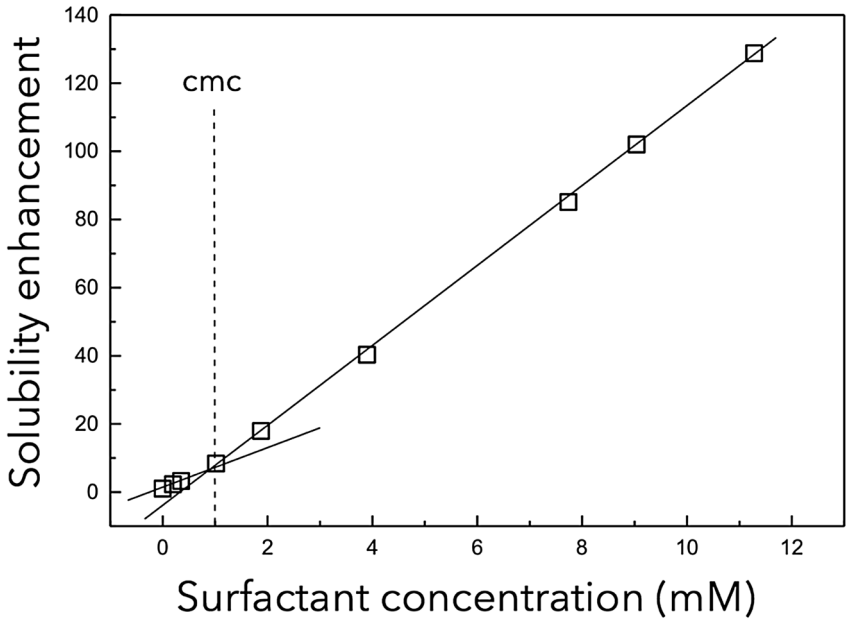

Fig. 25 Plot showing the solubilisation of naphthalene in aqueous solutions of the non-ionic surfactant P103 data taken from Ref. [69]

hydrocarbons and PAHs since they were identified as the primary risk drivers. About 351 tonnes of soil was excavated and placed in trenches where the soil was mixed with an aqueous solution of the non-ionic surfactant Tween 80. Figure 28 shows the chemical structure of Tween 80.

Measured initial soil concentrations of total petroleum hydrocarbons (TPH) ranged between 3000 to 17,000 mg kg^{-1}. Treatment with the surfactant solution was able to reduce TPH by between 55 to 93%. More importantly, measured TPH concentrations were reduced to levels below risk guidelines [72].

In situ remediation is implemented in very much in the same as ISCO. An aqueous surfactant solution is injected and flushed through the NAPL source zone and collected by a separate extraction well or wells. Essentially, the presence of micelles in the aqueous phase enhances the mass transfer of NAPL components from the trapped NAPL phase into the mobile aqueous phase [73] through the creation of an enhanced chemical potential gradient from the NAPL to the micelle via the aqueous phase. The solubilised components are then removed by the mobile aqueous phase. The process is thus in essence an augmented form of pump and treat whose effectiveness has been demonstrated in a number of field studies [74–76]. For example, in one demonstration a 1% surfactant solution was used to remove TCE from a sandy soil. Something like 21 pore volumes were used to remove the NAPL over a 4-year period [76]. It was estimated if only water was pumped through the system it would require 2000 pore volumes over 400 years to produce the same outcome.

In situ flushing works well if the hydraulic conductivity of the system is high and the system is relatively homogeneous. Other issues that arise that can compromise the efficacy of surfactant flushing are surfactant precipitation and surfactant adsorption to mineral surfaces. Hard water—water containing high levels of calcium ions—can cause surfactants to precipitate out of solution. For example, the solubility of sodium dodecyl sulphate below its cmc is controlled by the solubility product and calcium ion concentration [77]. Surfactant concentration in aqueous solution may also be depleted by adsorption to soil particle surfaces. Sub-surface surfaces, especially colloidal clay surfaces at circumneutral pH, are normally negatively charged. This arises from a number of different processes:

(1) isomorphous substitution such as the substitution of a Si^{4+} ion by an Al^{3+} ion;
(2) the deprotonation of OH groups attached to Al, Fe and Si atoms at clay edges;
(3) the ionisation of –OH and –COOH groups attached to soil organic matter.

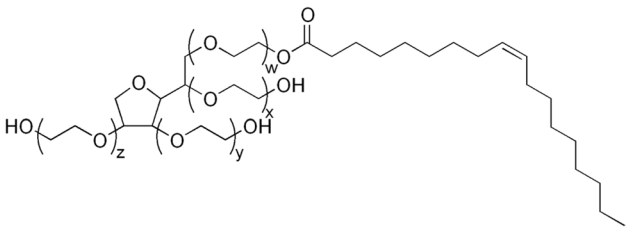

Fig. 28 Chemical structure of Tween 80—polyethylene glycol sorbitan monooleate. The sum of *w*, *x*, *y* and *z* is 20

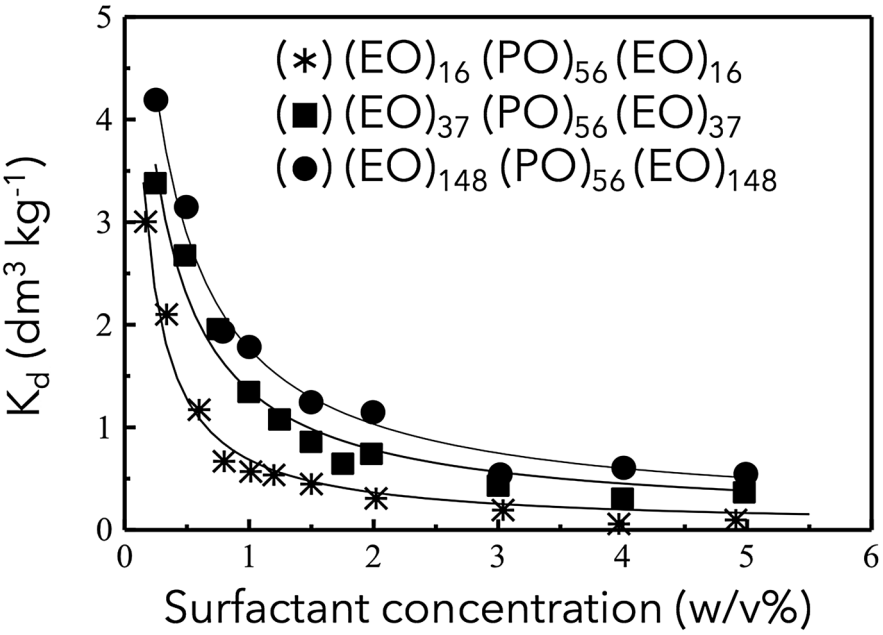

Fig. 27 K_d for the distribution of naphthalene between soil and water as a function of surfactant concentration for three EO-PO-EO block copolymeric surfactants. Data obtained from Ref. [71]

Cationic surfactants are readily adsorbed and as such are of little use for surfactant-enhanced groundwater remediation. Non-ionic surfactants, which comprise ethylene oxide oligomer chains, are also adsorbed to surface silanol (SiOH) groups through hydrogen bonding [78], though sorptive losses are dependent upon the nature of the solid phase. Bentonite, for example, a clay formed from volcanic ash can completely adsorb an ethylene oxide containing surfactant [79]. However, sand seems to have little adsorptive capacity for these surfactants [79].

Surfactant-enhanced remediation can prove to be expensive especially if using commercially sourced surfactants. Costs can be reduced by reusing the surfactant, which clearly requires the separation of the organic contaminant load from the surfactant.

A number of separation approaches have been investigated. Many have already been discussed in previous sections:

- Vapour stripping can be used to remove volatile or semi-volatile organic compounds [80] from the surfactant treatment stream. However, its effectiveness is compromised if foaming occurs as air is pumped through the surfactant solution. Instead of pumping, air can be drawn through the system through the application of a rough vacuum (a pressure ranging from atmospheric pressure down to 100 Pa). This can be used in conjunction with heat to separate the contaminant load from the surfactant [81]. This increases the separation effectiveness for low volatility organic compounds and reduces the amount of foaming [80, 82].
- Adsorption can be used to separate the contaminant load from the surfactant treatment stream through the use of a variety of adsorbents. These can include activated carbon and organo-clay materials [80].
- Oxidative degradation using *inter alia* Fenton's reaction and ozone [83].

Surfactant mobilisation

Residually trapped NAPL is immobilised in a porous medium by capillary forces. The scale of these forces is described by the right-hand term of the Laplace equation (Eq. 42)

$$P_e = \frac{2\sigma \mathrm{Cos}(\theta)}{r}, \tag{42}$$

where P_e is the displacement entry pressure (the pressure necessary to displace a NAPL droplet from a pore), σ is the interfacial tension, θ is the contact angle and r is the radius of the capillary, located in the porous medium, where the aqueous and NAPL phases are in contact.

Clearly if the contact angle (θ) could be increased or the interfacial tension (σ) decreased then the capillary trapping forces would be reduced and, under the right conditions, could be sufficiently reduced for mobilisation along a pressure gradient to occur. Surfactants are readily adsorbed at the NAPL/water interface because of their amphiphilic nature (i.e. the covalent linkage of hydrophobic and hydrophilic moieties) and as a consequence adsorption reduces the interfacial tension. Thus, surfactants can significantly reduce the pressure gradient necessary to mobilise a trapped NAPL in a porous medium.

Engineers define three dimensionless numbers to characterise the trapping and mobilisation of a NAPL [73, 84]:

- The *capillary number* (N_C), which is the ratio of the of the viscous force generated by flowing groundwater and the capillary force generated at the curved interface between water and NAPL at a pore throat.

$$N_C = \frac{q_w \eta_w}{\sigma_{NW} \mathrm{Cos}(\theta)}, \tag{43}$$

  where q_w is the Darcy velocity (or flux), which is the volume of water through unit cross-sectional of porous medium in unit time and is given by $K_H \Delta h / \Delta l$ (see Eq. 16); η_w is the viscosity of water; the subscripts N and W refer to NAPL and water respectively.
- The *Bond number* (N_B), which is the ratio of the buoyancy force to the capillary force:

$$N_B = \frac{\alpha\ \Delta\rho\ g\ k_i\ k_{rw}}{\sigma_{NW} \mathrm{Cos}(\theta)}, \tag{44}$$

  where α is the slope of flow relative to the horizontal axis $\Delta\rho$ is the density difference between the NAPL and water, g is the acceleration due to gravity, and k_i the intrinsic permeability of the porous medium—this is the permeability of the system independent of the fluid and determined by the architecture of the porous medium and k_{rw} is the relative permeability of the aqueous phase that is the permeability of the system to water flow when a second fluid phase is present.
- Finally, the *trapping number* (N_T), which is defined as the vector summation of the *Bond* and *capillary numbers*.

$$N_T = \sqrt{N_C^2 + 2N_C N_B \mathrm{Sin}(\alpha) + N_B^2}. \tag{45}$$

It has been demonstrated that the trapping number must exceed a critical value for NAPL to be mobilised. Several independent experiments suggest that the critical trapping number is in the range of 1.5×10^{-5} and 5×10^{-5} [73].

Of course, mobilisation may actually be a problem when dealing with DNAPLs. If mobilised without taking precautions, trapped DNAPLs will tend to sink further in the subsurface making them more difficult to deal with and may in fact create a much wider spread environmental challenge. Thus, engineered soil flushing of DNAPLs is very often designed to enhance solubilisation but to suppress mobilisation [85].

The use of aqueous surfactant solutions to displace trapped NAPLs from a porous medium is referred to as immiscible displacement. Immiscible displacement using surfactant solutions was first developed by petroleum engineers to increase the productivity of petroleum extraction from oil reservoirs. Its use was justified when the price of crude oil was sufficiently high to make it cost effective. However, it does not usually extract all the emplaced oil. Whilst this may make economic sense for the petroleum industry it does not necessarily reduce risk posed by NAPL-impacted environments, though it may reduce the longevity of the source zone. Thus, immiscible displacement only makes remedial sense if it can significantly reduce risk.

One issue that can be addressed here is that surfactants may be added to organic solvents to improve their end use in industrial applications. However, surfactants present in solvents like trichloroethene will alter their wetting properties as shown in Fig. 29

Quartz surfaces are usually hydrophilic. Thus, when TCE is placed on a quartz surface as shown in Fig. 29 in a water-filled environment, the TCE will tend to bead up, as shown in the left-hand photograph in Fig. 29. The TCE drop, shown in the right-hand photograph of Fig. 29, is, on the other hand, loaded with surfactant and as a result spreads across the quartz surface. This occurs because the cationic head group of the surfactant is adsorbed to the quartz surface, which permits the hexadecyl chains to embed themselves into the TCE. By this mechanism, the TCE drop spreads over the quartz surface. Such changes in wetting can make it much harder to remove the NAPL [86].

Microemulsion formation

Emulsions are formed by the fine dispersion of one immiscible phase in a second continuous phase. They are thermodynamically unstable. One familiar example of emulsion formation is provided by solvent extraction wherein an organic solvent is used to extract a hydrophobic solute from an aqueous solution. The emulsion is formed by vigorous agitation and rapidly separates (we use the term breaks) into two phases once agitation has ceased. The mechanism by which this emulsion breaks is via the coalescence of the dispersed phase droplets. A free energy penalty arises from the interfacial tension that exists at the interface between the immiscible water and organic liquid phases. The free energy penalty is given by $\sigma_{NW}\Delta A$ [87] where σ_{NW} is the water/NAPL interfacial tension and ΔA the increase in interfacial area. Clearly the greater the number of droplets is the greater the magnitude of interfacial areal contact and thus the greater the free energy penalty. In the absence of a droplet stabilisation mechanism coalescence of two droplets that come into contact is thermodynamically favoured.

Surfactant adsorption at the droplet interface reduces the interfacial tension and thus reduces the free energy penalty associated with droplet formation. However, the presence of surfactant at the droplet interface can also make a contribution to droplet stabilisation. If the surfactant is ionic then coalescence is hindered by the coulombic repulsion arising from the charged headgroups at the surface of the organic liquid drop [64]. If the surfactant is non-ionic then the hydrophilic parts of the surfactant molecules—which are very often polymeric—stabilise the dispersed organic

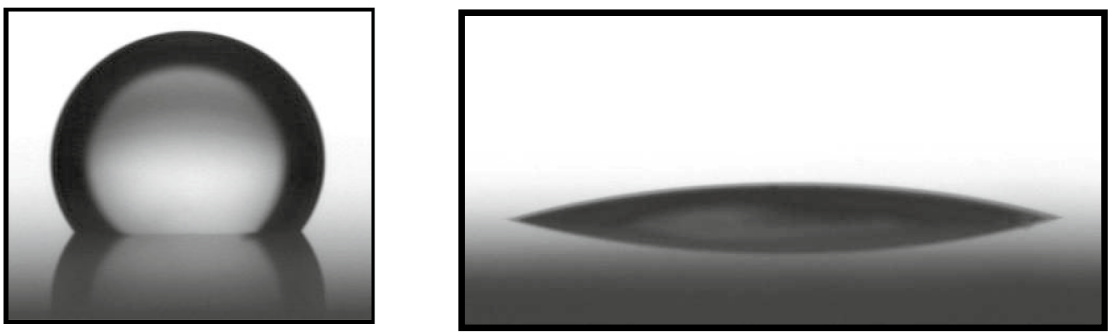

Fig. 29 Effect of the cationic surfactant hexadecyltrimethyl ammonium bromide dissolved in trichloroethene (TCE) on the wetting properties of trichloroethene on quartz in a water-filled environment

liquid droplets through the osmotic gradient that is created by the local increase in concentration of the hydrophilic chains when two droplets come together [88]. Despite the free energy penalty reduction and the stabilisation arising from surfactant adsorption, emulsion formation for this ternary component system still requires the input of energy, which suggests that flushing a surfactant solution through a source zone will form an emulsion with difficulty if at all.

However, it is possible to formulate systems that spontaneously form emulsions. These thermodynamically stable, optically transparent emulsions are called microemulsions. The use of microemulsions for tertiary oil recovery has been extensively investigated as a means of increasing the yield of petroleum from oil reservoirs [89]. The problems that microemulsions address in petroleum engineering—namely displacing crude oil trapped in tight formation pores—are the same as those provided by the presence of NAPLs in soils and rocks. Microemulsions can be produced by the suitable formulation of a ternary component system—water, NAPL and surfactant at an appropriate temperature and pressure. However, for the remediation of NAPL-impacted environments it may be more convenient to use additional components such as salt, alcohol, co-surfactant or an organic solvent [90]. Figure 30 shows a series of microemulsions formed by the addition of sodium chloride to an aqueous phase that already contains the anionic surfactant sodium dodecyl sulphate (SDS). The organic phase is a coal tar sample obtained from a former coal gas manufacturing site based in the English Midlands. In test tube 1 the system has separated into two phases, a lower coal tar phase and an upper NAPL-in-water microemulsion phase. This upper phase consists of swollen micelles and is described as a Winsor type 1 microemulsion [91]. The role of sodium chloride is apparently two-fold. The presence of sodium chloride reduces the solubility of the dodecyl chains present in the SDS molecule and thus increases their surface activity, i.e. their adsorption at interfaces. Second, the increase in ionic strength provided by the presence of sodium chloride also means that the SDS molecules adsorbed at an interface are able to pack closer together because of the reduced electrostatic repulsion between the sulphate head groups. This may help to produce smaller, more tightly curved micelles, which increases the transparency of the emulsion, though it must be confessed that coal tar emulsions do not lend themselves well to transparency. In test tube 4, the salinity is so great that we obtain inverted micelles, which are more soluble in the NAPL phase. As a result, we obtain a water-in-coal tar microemulsion, which is the lower phase. This is called a Winsor type 2 microemulsion.

In test tubes 2 and 3, the system splits into three phases, an upper water phase, a lower coal tar phase and a middle phase comprising the microemulsion. This type of microemulsion is called a Winsor type 3. Studies show that the middle phase can have a very low interfacial tension, and the size and size distribution of the dispersed phase particles can be small [92]. Such properties are enormously helpful in aiding the removal of NAPL. The aim of environmental engineers is to formulate the system such that the size of the middle phase is as large as possible. The reader can observe that the size of the middle phase in tube 2 (in Fig. 30) is greater than that in tube 3. There are times when the system is formulated so that the middle phase is the only phase that is formed. This is called a Winsor type 4 system. There have been several field studies which have demonstrated that micro-emulsion flooding can be very effective in removing NAPL from sub-surface locations [90, 93].

Natural attenuation

So far, we have examined chemical and/or physical intervention as the means by which the risk posed by pollutants transported, from a source zone, through groundwater to a receptor can be either mitigated or reduced to an acceptable level. Intervention is costly and in some cases unnecessary since natural physical, chemical and microbiological processes may reduce contaminant concentrations to safe levels at regulatory compliance points (RCPs) such as water supply wells. Reliance upon naturally occurring phenomena is described as natural attenuation (NA). The focus of NA is not on contaminant concentrations that emerge from a source zone which may be greatly in excess of guideline water quality values, but on the concentrations at RCPs. These are points where breaches of water quality regulations will almost certainly lead to legal penalties. NA is therefore an attractive remedial option, though it does need

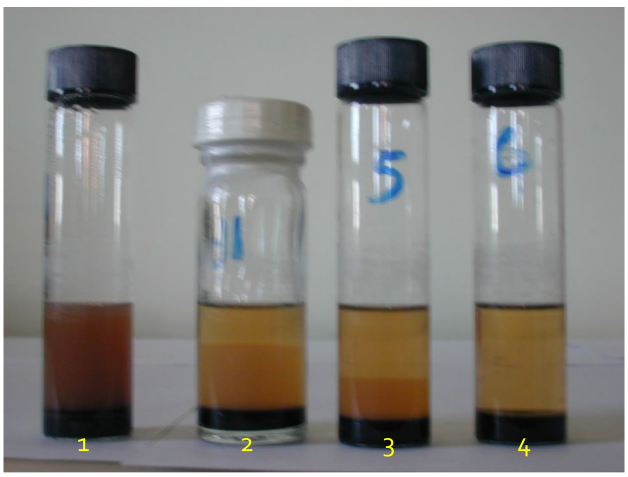

Fig. 30 Microemulsion formation for a water/coal tar/sodium dodecyl sulphate/sodium chloride system. The amount of each component is constant except for the concentration of sodium chloride, which increases from test bottle 1 through to 4

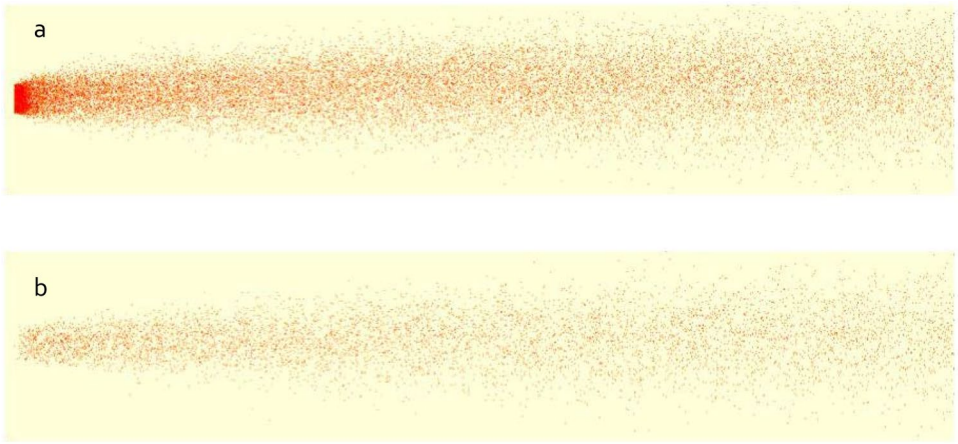

Fig. 31 Impact of partial mass removal upon the **a** contaminant plume. In the bottom diagram **b** the mass of NAPL has been reduced by 90%. It is assumed that the contaminant is recalcitrant. Thus, the first-order degradation rate constant is set equal to 0

Fig. 32 Simulation of the impact of degradation upon a contaminant plume. The conditions for the simulations in the upper (**a**) and lower (**b**) diagrams are the same as those in Fig. 31 with the exception that assumed degradation rate constant is set equal to 0.01 t^{-1} where t is the simulation time unit

to be established that it can provide the necessary protection of RCPs.

Processes that contribute to NA include [23, 94]:

- Dispersion (given by the *D* term in Eq. 11) describes the spreading out of the pollutant as it migrates in the flowing groundwater.
- Volatilisation—the transfer of a solute from the aqueous phase to the vapour phase and described by the Henry's law constant (see Eq. 6).
- Dilution—when the contaminant plume intersects a water supply well the contaminant is drawn up in the well. However, the well also draws in uncontaminated water, which has the effect of diluting the contaminant concentration emerging from the well head.
- Retardation—as a plume is growing the retardation of the contaminant velocity through interaction with organic carbon present on the surface of soil and rock surfaces reduces the rate at which the plume advances.
- Microbiological degradation—many organic contaminants are used as electron donors by microbiological organisms. Oxidation of the pollutants can therefore be an important part of microbiological metabolism. In some other cases the contaminant may act as an electron acceptor.

As we have emphasised previously a contaminant plume does not grow indefinitely but actually reaches a steady-state length when the influx of contaminant from the source zone is balanced by natural attenuation processes. Unfortunately, non-engineered microbial-mediated degradation—which is likely to be the most important NA process—is slow. As such, it is unlikely to be sufficient to reduce the plume length so as to prevent the plume infringing an RCP in cases where NAPL is present. If the rate of influx is reduced then plume length is reduced as long as the rate of natural attenuation is not altered. Influx is certainly reduced if the NAPL source zone is removed and in many cases NA will be sufficient to "mop up" the aqueous phase contaminant load so that

the reduced plume does not breach a regulatory limit at a compliance point. However, nearly all engineered NAPL removal systems such as surfactant flooding are defeated by the heterogeneity of the sub-surface environment. At best, we may only achieve partial mass removal. However, even partial mass removal coupled with NA may be sufficient to protect an RCP. We can demonstrate this using the simple stochastic model, which was introduced in Ref. [2]. The results of the simulations are shown in Figs. 31 and 32.

The impact of partial mass removal without NA is shown in Fig. 31. It is clear that in the Fig. 31b where the source zone has been reduced by 90% that the plume intensity is reduced. Whether this reduction is sufficient to protect an environmental receptor is moot. However, in Fig. 32 it is clear that with partial mass removal coupled with NA, the concentration of contaminant in the plume is reduced sufficiently that it should pose a negligible risk to a receptor situated some distance from the source zone.

It is, of course, possible that even when there is no mass removal of the source zone the degradation rate can be improved sufficiently to protect a receptor. For example, the microbially mediated degradation of common electron donors like petroleum hydrocarbons is normally limited by the absence of suitable electron acceptors like oxygen. However, sub-surface microbiota are facultative anaerobes, which means that they can use other electron acceptors, like sulphate, nitrate, iron(III) and hydrogen carbonate ions. If the concentration of oxygen is limiting the rate of degradation of the contaminant present in the plume then it can be introduced via pumping (biosparging—see the section on air sparging) or through the use of oxygen release compound [95]. Oxygen release compound is a patented proprietary formulation containing magnesium peroxide. Increasing the electron acceptor concentration is referred to as biostimulation. We could also increase the numbers of or introduce more suitable microbial consortia. This is referred to as bioaugmentation.

In some cases, the target contaminant compound is an electron acceptor. Chlorinated hydrocarbon solvents like trichloroethene and trichloromethane fall into this category. The microbiological genus *Dehalococcoides* has been successfully used to reduce chlorinated ethenes through dehydrochlorination down to ethene and ethane [96]. To accomplish this the redox conditions of groundwater environment are made reducing. This is done via the addition of an electron acceptor. The SABRE (Source Area BioREmediation) project, completed in the UK, tested a number of electron donors including soya bean oil, hexanol and butyl ethanoate in a series of microcosm experiments with dehalorespiring bacteria [97].

The question naturally arises: do we rely upon NA or do we use biostimulation and/or bioaugmentation? In depth site characterisation coupled with a functional conceptual model of how the pollutant behaves on site and a proper risk assessment will help answer the question.

Final remarks

The initial aim of this text has been to show how toxicological data can be used in risk assessment to set permissible levels for NAPL-derived contaminants in groundwater. Next we have examined how contaminated groundwater systems can be treated so as to reduce environmentally challenging VOC concentrations to acceptable levels. We have tried to elucidate the essential physics and chemistry of a number of remediation technologies. The choice of which technology to use is determined by the nature of the problem. If NAPL is present then an on-site engineer's initial concern may be with preventing any mobile NAPL from migrating off-site. If NAPL is present but immobile then removal of the source zone or containment and/or treatment of the plume may become the next concern. For a NAPL source zone surfactant flooding may be a suitable treatment, but it is inappropriate for treating VOCs dissolved in groundwater—they are already present in the mobile groundwater. For a contaminant plume air sparging is likely to be successful when dealing with petroleum hydrocarbons but not good for VOCs with low Henry's law constants. There are a number of treatments that have not been dealt with, for example heating to volatilise VOCs and smouldering to slowly, flamelessly combust NAPLs. There is clearly scope for the development of further treatments by chemists and chemical engineers.

References

1. Kueper BH, Wealthall GP, Smith JWN, Leharne SA, Lerner DN (2003) An illustrated handbook of DNAPL transport and fate in the subsurface. Environment Agency, Bristol
2. Leharne S (2019) Transfer phenomena and interactions of non-aqueous phase liquids in soil and groundwater. ChemTexts 5(1):5. https://doi.org/10.1007/s40828-019-0079-2

3. Bosgra S, Bos PM, Vermeire TG, Luit RJ, Slob W (2005) Probabilistic risk characterization: an example with di(2-ethylhexyl) phthalate. Regul Toxicol Pharmacol 43(1):104–113. https://doi.org/10.1016/j.yrtph.2005.06.008
4. Dankovic DA, Naumann BD, Maier A, Dourson ML, Levy LS (2015) The scientific basis of uncertainty factors used in setting occupational exposure limits. J Occup Environ Hyg 12(suppl 1):S55–S68. https://doi.org/10.1080/15459624.2015.1060325
5. Masters GM, Wendell PE (2014) Introduction to environmental engineering and science. Pearson Education Limited, Harlow
6. Pohl H, DeRosa C, Holler J (1995) Public health assessment for dioxins exposure from soil. Chemosphere 31(1):2437–2454. https://doi.org/10.1016/0045-6535(95)00114-n
7. Hites RA (2011) Dioxins: an overview and history. Environ Sci Technol 45(1):16–20. https://doi.org/10.1021/es1013664
8. White KL Jr, Lysy HH, McCay JA, Anderson AC (1986) Modulation of serum complement levels following exposure to polychlorinated dibenzo-p-dioxins. Toxicol Appl Pharmacol 84(2):209–219. https://doi.org/10.1016/0041-008x(86)90128-6
9. Janeway CA, Travers P, Walport M, Shlomchik M (2001) Immunobiology: the immune system in health and disease, 5th edn. Garland Sciene, New York
10. Altshuler B (1981) Modeling of dose-response relationships. Environ Health Perspect 42:23–27. https://doi.org/10.1289/ehp.814223
11. Zeise L, Wilson R, Crouch EA (1987) Dose-response relationships for carcinogens: a review. Environ Health Perspect 73:259–306. https://doi.org/10.1289/ehp.8773259
12. Anderson EL (1983) Quantitative approaches in use to assess cancer risk. Risk Anal 3(4):277–295. https://doi.org/10.1111/j.1539-6924.1983.tb01396.x
13. European Chemicals Agency Carbon Tetrachloride. https://echa.europa.eu/registration-dossier/-/registered-dossier/14940/4/9
14. United States Environmental Protection Agency Carbon tetrachloride CASRN 56-23-5. https://cfpub.epa.gov/ncea/iris2/chemicalLanding.cfm?substance_nmbr=20
15. Cancer Research UK. https://www.cancerresearchuk.org/health-professional/cancer-statistics/incidence/all-cancers-combined. Accessed 19 August 2021
16. Kumari M, Gupta SK, Mishra BK (2015) Multi-exposure cancer and non-cancer risk assessment of trihalomethanes in drinking water supplies—a case study of Eastern region of India. Ecotoxicol Environ Saf 113:433–438. https://doi.org/10.1016/j.ecoenv.2014.12.028
17. Smith EB (1990) Basic chemical thermodynamics. Oxford Chemistry Series, 4th edn. Clarendon Press, Oxford
18. Mackay D (1991) Multimedia environmental models: the fugacity approach. Technology and Environmental Health Series. Lewis Publishers Inc, Chelsea
19. United States Environmental Protection Agency Benzene; CASRN 71-43-2. https://cfpub.epa.gov/ncea/iris2/chemicalLanding.cfm?substance_nmbr=276
20. World Health Organisation (2017) Guidelines for drinking-water quality, 4th edn, incorporating the 1st addendum. WHO. https://www.who.int/water_sanitation_health/publications/drinking-water-quality-guidelines-4-including-1st-addendum/en/
21. Yao Y, Pennell KG, Suuberg E (2011) Vapor intrusion in urban settings: effect of foundation features and source location. Procedia Environ Sci 4:245–250. https://doi.org/10.1016/j.proenv.2011.03.029
22. National Research Council (2005) Contaminants in the subsurface: source zone assessment and remediation. The National Academies Press, Washington, DC. https://doi.org/10.17226/11146
23. Wilson RD, Thornton SF, Lerner DN (2008) Forecasting natural attenuation as a risk-based groundwater remediation strategy, chapter 7.2. In: Groundwater science and policy: an international overview. The Royal Society of Chemistry, pp 421–453. https://doi.org/10.1039/9781847558039-00421
24. Fetter CW (1994) Applied hydrogeology. Prentice Hall Inc., Upper Saddle River
25. Delgado JMPQ (2007) Longitudinal and transverse dispersion in porous media. Chem Eng Res Des 85(9):1245–1252. https://doi.org/10.1205/cherd07017
26. National Center for Biotechnology Information. PubChem Database. Chloroform, CID=6212. https://pubchem.ncbi.nlm.nih.gov/compound/Chloroform. Accessed 21 May 2020
27. United States Environmental Protection Agency National Primary Drinking Water Regulations. https://www.epa.gov/sites/production/files/2016-06/documents/npwdr_complete_table.pdf
28. Mackay DM, Roberts PV, Cherry JA (1985) Transport of organic contaminants in groundwater. Environ Sci Technol 19(5):384–392. https://doi.org/10.1021/es00135a001
29. Smith WO, Sayre AN (1964) Turbulence in ground-water flow. Professional Paper. United States Geological Survey, Washington DC. https://doi.org/10.3133/pp402E
30. Allen-King RM, Grathwohl P, Ball WP (2002) New modeling paradigms for the sorption of hydrophobic organic chemicals to heterogeneous carbonaceous matter in soils, sediments, and rocks. Adv Water Resour 25(8):985–1016. https://doi.org/10.1016/S0309-1708(02)00045-3
31. Weber WJ, LeBoeuf EJ, Young TM, Huang W (2001) Contaminant interactions with geosorbent organic matter: insights drawn from polymer sciences. Water Res 35(4):853–868. https://doi.org/10.1016/S0043-1354(00)00339-0
32. Li L, Quinlivan PA, Knappe DRU (2002) Effects of activated carbon surface chemistry and pore structure on the adsorption of organic contaminants from aqueous solution. Carbon 40(12):2085–2100. https://doi.org/10.1016/S0008-6223(02)00069-6
33. Mackay DM, Cherry JA (1989) Groundwater contamination—pump-and-treat remediation. 2. Environ Sci Technol 23(6):630–636
34. United States Environmental Protection Agency (2012) A citizen's guide to pump and treat. https://semspub.epa.gov/work/HQ/158717.pdf
35. Gillham RW, O'Hannesin SF (1994) Enhanced degradation of halogenated aliphatics by zero-valent iron. Ground Water 32(6):958–967
36. Vogel TM, Criddle CS, McCarty PL (1987) ES Critical Reviews: transformations of halogenated aliphatic compounds. Environ Sci Technol 21(8):722–736. https://doi.org/10.1021/es00162a001
37. Matheson LJ, Tratnyek PG (1994) Reductive dehalogenation of chlorinated methanes by iron metal. Environ Sci Technol 28(12):2045–2053. https://doi.org/10.1021/es00061a012
38. United States Environmental Protection Agency (1998) Permeable reactive barrier technologies for contaminant remediation. USEPA. https://clu-in.org/download/rtdf/prb/reactbar.pdf
39. Mayer KU, Blowes DW, Frind EO (2001) Reactive transport modeling of an in situ reactive barrier for the treatment of hexavalent chromium and trichloroethylene in groundwater. Water Resour Res 37(12):3091–3103. https://doi.org/10.1029/2001wr000234
40. Tosco T, Petrangeli Papini M, Cruz Viggi C, Sethi R (2014) Nanoscale zerovalent iron particles for groundwater remediation: a review. J Clean Prod 77:10–21. https://doi.org/10.1016/j.jclepro.2013.12.026
41. Obiri-Nyarko F, Grajales-Mesa SJ, Malina G (2014) An overview of permeable reactive barriers for in situ sustainable groundwater remediation. Chemosphere 111:243–259. https://doi.org/10.1016/j.chemosphere.2014.03.112
42. Firdous R, Devlin JF (2018) Surface carbon influences on the reductive transformation of TCE in the presence of granular iron. J

Hazard Mater 347:31–38. https://doi.org/10.1016/j.jhazmat.2017.12.043
43. Wilkin RT, Puls RW, Sewell GW (2002) Long term performance of permeable reactive barriers using zero-valent iron: an evaluation at two sites. USEPA. https://www.researchgate.net/publication/235051894_Long-term_Performance_of_Permeable_Reactive_Barriers_Using_Zero-valent_Iron_An_Evaluation_at_Two_Sites
44. Thiruvenkatachari R, Vigneswaran S, Naidu R (2008) Permeable reactive barrier for groundwater remediation. J Ind Eng Chem 14(2):145–156. https://doi.org/10.1016/j.jiec.2007.10.001
45. Powell RM, Puls RW, Hightower SK, Sabatini DA (1995) Coupled iron corrosion and chromate reduction: mechanisms for subsurface remediation. Environ Sci Technol 29(8):1913–1922. https://doi.org/10.1021/es00008a008
46. Schnarr M, Truax C, Farquhar G, Hood E, Gonullu T, Stickney B (1998) Laboratory and controlled field experiments using potassium permanganate to remediate trichloroethylene and perchloroethylene DNAPLs in porous media. J Contam Hydrol 29(3):205–224. https://doi.org/10.1016/S0169-7722(97)00012-0
47. Watts RJ, Teel AL (2006) Treatment of contaminated soils and groundwater using ISCO. J Hazard Toxic Radioact Waste 10(1):2–9. https://doi.org/10.1061/(ASCE)1090-025X(2006)10:1(2)
48. Li H, Han Z, Qian Y, Kong X, Wang P (2019) In situ persulfate oxidation of 1,2,3-trichloropropane in groundwater of North China Plain. Int J Environ Res Public Health 16(15):2752. https://doi.org/10.3390/ijerph16152752
49. Malik SN, Ghosh PC, Vaidya AN, Mudliar SN (2020) Hybrid ozonation process for industrial wastewater treatment: principles and applications: a review. J Water Process Eng 35:101193. https://doi.org/10.1016/j.jwpe.2020.101193
50. ITRC (Interstate Technology and Regulatory Council) (2005) Technical and regulatory guidance for in-situ chemical oxidation of contaminated soil and groundwater 2nd edn, ISCO-2. https://www.itrcweb.org/GuidanceDocuments/ISCO-2.pdf
51. Speight JC (2018) Reaction mechanisms in environmental engineering: analysis and prediction. Butterworth-Heinemann, Cambridge
52. Huang K-C, Hoag GE, Chheda P, Woody BA, Dobbs GM (2002) Kinetics and mechanism of oxidation of tetrachloroethylene with permanganate. Chemosphere 46(6):815–825. https://doi.org/10.1016/S0045-6535(01)00186-2
53. Yan YE, Schwartz FW (1999) Oxidative degradation and kinetics of chlorinated ethylenes by potassium permanganate. J Contam Hydrol 37(3):343–365. https://doi.org/10.1016/S0169-7722(98)00166-1
54. Chokejaroenrat C, Comfort S, Sakulthaew C, Dvorak B (2014) Improving the treatment of non-aqueous phase TCE in low permeability zones with permanganate. J Hazard Mater 268:177–184. https://doi.org/10.1016/j.jhazmat.2014.01.007
55. Crimi M, Ko S (2009) Control of manganese dioxide particles resulting from in situ chemical oxidation using permanganate. Chemosphere 74(6):847–853. https://doi.org/10.1016/j.chemosphere.2008.09.074
56. Ma M (2012) The dispersive effect of sodium hexametaphosphate on kaolinite in saline water. Clays Clay Miner 60(4):405–410. https://doi.org/10.1346/CCMN.2012.0600406
57. Fenton HJH (1894) LXXIII—oxidation of tartaric acid in presence of iron. J Chem Soc Trans 65:899–910. https://doi.org/10.1039/CT8946500899
58. Anbar M, Meyerstein D, Neta P (1966) The reactivity of aromatic compounds toward hydroxyl radicals. J Phys Chem 70(8):2660–2662. https://doi.org/10.1021/j100880a034
59. Qiang Z, Ben W, Huang C-P (2008) Fenton process for degradation of selected chlorinated aliphatic hydrocarbons exemplified by trichloroethylene, 1,1-dichloroethylene and chloroform. Fron Environ Sci Eng 2(4):397. https://doi.org/10.1007/s11783-008-0074-0
60. McCray JE (2000) Mathematical modeling of air sparging for subsurface remediation: state of the art. J Hazard Mater 72(2):237–263. https://doi.org/10.1016/S0304-3894(99)00142-9
61. Guo Z, Roache NF (2003) Overall mass transfer coefficient for pollutant emissions from small water pools under simulated indoor environmental conditions. Ann Occup Hyg 47(4):279–286. https://doi.org/10.1093/annhyg/meg035
62. Chao K-P, Ong Say K, Protopapas A (1998) Water-to-air mass transfer of VOCs: laboratory-scale air sparging system. J Environ Eng 124(11):1054–1060. https://doi.org/10.1061/(ASCE)0733-9372(1998)124:11(1054)
63. Fanchi JR (2018) Fluid properties and model initialization, chapter 6. In: Fanchi JR (ed) Principles of applied reservoir simulation, 4th edn. Gulf Professional Publishing, pp 101–120. https://doi.org/10.1016/B978-0-12-815563-9.00006-9
64. Hunter RJ (1995) Foundations of colloid science, vol 1. Oxford University Press, Oxford
65. Berry MV (1971) The molecular mechanism of surface tension. Phys Educ 6(2):79
66. Aston MS (1993) The study of surfactant monolayers by surface pressure–area measurement. Chem Soc Rev 22(1):67–71. https://doi.org/10.1039/CS9932200067
67. Tanford C (1973) The hyrdophobic effect: formation of micelles and biological membranes. Wiley, New York
68. Rosen MJ (1989) Surfactants and inteterfacial phenomena, 2nd edn. Wiley, New York
69. Paterson IF, Chowdhry BZ, Leharne SA (1999) Investigations of naphthalene solubilization in aqueous solutions of ethylene oxide-b-propylene oxide-b-ethylene oxide copolymers. Langmuir 15(19):6187–6194
70. Paterson IF, Chowdhry BZ, Leharne SA (1999) Polycyclic aromatic hydrocarbon extraction from a coal tar-contaminated soil using aqueous solutions of nonionic surfactants. Chemosphere 38(13):3095–3107
71. Paterson IF, Chowdhry BZ, Leharne SA (1999) Predicting surfactant modified soil/water distribution coefficients using micellar HPLC. Chemosphere 38(2):263–273
72. Iturbe R, Flores C, Chavez C, Bautista G, Torres LG (2004) Remediation of contaminated soil using soil washing and biopile methodologies at a field level. J Soil Sediment 4(2):115. https://doi.org/10.1007/BF02991055
73. Huo L, Liu G, Yang X, Ahmad Z, Zhong H (2020) Surfactant-enhanced aquifer remediation: mechanisms, influences, limitations and the countermeasures. Chemosphere 252:126620. https://doi.org/10.1016/j.chemosphere.2020.126620
74. Fountain JC, Starr RC, Middleton T, Beikirch M, Taylor C, Hodge D (1996) A controlled field test of surfactant-enhanced aquifer remediation. Groundwater 34(5):910–916. https://doi.org/10.1111/j.1745-6584.1996.tb02085.x
75. Abdul AS, Ang CC (1994) In-situ surfactant washing of polychlorinated-biphenyls and oils from a contaminated field site—phase-II pilot-study. Ground Water 32(5):727–734
76. Mulligan CN, Yong RN, Gibbs BF (2001) Surfactant-enhanced remediation of contaminated soil: a review. Eng Geol 60(1–4):371–380
77. Baviere M, Bazin B, Aude R (1983) Calcium effect on the solubility of sodium dodecyl sulfate in sodium chloride solutions.

J Colloid Interface Sci 92(2):580–583. https://doi.org/10.1016/0021-9797(83)90179-0
78. Paterson IF, Chowdhry BZ, Carey PJ, Leharne SA (1999) Examination of the adsorption of ethylene oxide-propylene oxide triblock copolymers to soil. J Contam Hydrol 40(1):37–51
79. Hagenhoff K, Dong JF, Chowdhry B, Torres L, Leharne S (2012) The impact of four ethylene oxide-propylene oxide block copolymers on the surface tension of dispersions of soils and minerals in water. Phys Chem Earth 37–39:58–64. https://doi.org/10.1016/J.Pce.2010.11.002
80. Trellu C, Pechaud Y, Oturan N, Mousset E, van Hullebusch ED, Huguenot D, Oturan MA (2021) Remediation of soils contaminated by hydrophobic organic compounds: how to recover extracting agents from soil washing solutions? J Hazard Mater 404:124–137. https://doi.org/10.1016/j.jhazmat.2020.124137
81. Choori UN, Scamehorn JF, O'Haver JH, Harwell JH (1998) Removal of volatile organic compounds from surfactant solutions by flash vacuum stripping in a packed column. Ground Water Monit Remediat 18(4):157–165. https://doi.org/10.1111/j.1745-6592.1998.tb00175.x
82. Lipe KM, Sabatini DA, Hasegawa MA, Harwell JH (1996) Micellar-enhanced ultrafiltration and air stripping for surfactant-contaminant separation and surfactant reuse. Ground Water Monit Remediat 16(1):85–92. https://doi.org/10.1111/j.1745-6592.1996.tb00574.x
83. Trellu C, Mousset E, Pechaud Y, Huguenot D, van Hullebusch ED, Esposito G, Oturan MA (2016) Removal of hydrophobic organic pollutants from soil washing/flushing solutions: a critical review. J Hazard Mater 306:149–174. https://doi.org/10.1016/j.jhazmat.2015.12.008
84. West CC, Harwell JH (1992) Surfactants and subsurface remediation. Environ Sci Technol 26(12):2324–2330
85. Fountain JC, Klimek A, Beikirch MG, Middleton TM (1991) The use of surfactants for in situ extraction of organic pollutants from a contaminated aquifer. J Hazard Mater 28(3):295–311
86. Powers SE, Anckner WH, Seacord TF (1996) Wettability of NAPL-contaminated sands. J Environ Eng-ASCE 122(10):889–896
87. Hiemenz PC, Rajagopalan R (1997) Principles of colloid and surface chemistry, 3rd edn. Marcel Dekker Inc., New York
88. Tadros T (2009) Polymeric surfactants in disperse systems. Adv Colloid Interface 147–148:281–299. https://doi.org/10.1016/j.cis.2008.10.005
89. Li Z, Xu D, Yuan Y, Wu H, Hou J, Kang W, Bai B (2020) Advances of spontaneous emulsification and its important applications in enhanced oil recovery process. Adv Colloid Interface 277:102119. https://doi.org/10.1016/j.cis.2020.102119
90. Martel R, Gélinas PJ, Desnoyers JE (1998) Aquifer washing by micellar solutions: 1: optimization of alcohol–surfactant–solvent solutions. J Contam Hydrol 29(4):319–346. https://doi.org/10.1016/S0169-7722(97)00029-6
91. Winsor PA (1954) Solvent properties of amphiphilic molecules. Butterworth's Scientific Publications, London
92. Nordiyana MSW, Khalil M, Jan BM, Ali BS, Tong CW (2016) Formation and phase behavior of winsor type III *Jatropha curcas*-based microemulsion systems. J Surfactant Deterg 19(4):701–712. https://doi.org/10.1007/s11743-016-1814-y
93. Sharma P, Kostarelos K, Lenschow S, Christensen A, de Blanc PC (2020) Surfactant flooding makes a comeback: results of a full-scale, field implementation to recover mobilized NAPL. J Contam Hydrol 230:103602. https://doi.org/10.1016/j.jconhyd.2020.103602
94. Mulligan CN, Yong RN (2004) Natural attenuation of contaminated soils. Environ Int 30(4):587–601
95. Koenigsberg SS, Sandefur CA (1999) The use of oxygen release compound for the accelerated bioremediation of aerobically degradable contaminants: the advent of time-release electron acceptors. Remed J 10(1):3–29. https://doi.org/10.1002/rem.3440100103
96. Saiyari DM, Chuang H-P, Senoro DB, Lin T-F, Whang L-M, Chiu Y-T, Chen Y-H (2018) A review in the current developments of genus *Dehalococcoides*, its consortia and kinetics for bioremediation options of contaminated groundwater. Sustain Environ Res 28(4):149–157. https://doi.org/10.1016/j.serj.2018.01.006
97. Harkness M, Fisher A, Royer R, Possolo A, Lee MH, Mack EE, Payne JA, Major DW, Roberts J, Dworatzek S, Mao X (2006) Project SABRE (Source Area BioREmediation) Progress Report: results of a laboratory microcosm study to determine the potential for bioremediation of chlorinated solvent DNAPL source areas. https://www.claire.co.uk/component/phocadownload/category/11-research-bulletins?d. Accessed 17 Nov 2020